

2014

Novel Strategies for the Purification and Inhibition of Protein-Tyrosine Kinases

Alexander Brown IV
University of Rhode Island, abro4576@gmail.com

Follow this and additional works at: https://digitalcommons.uri.edu/oa_diss

Terms of Use

All rights reserved under copyright.

Recommended Citation

Brown, Alexander IV, "Novel Strategies for the Purification and Inhibition of Protein-Tyrosine Kinases" (2014). *Open Access Dissertations*. Paper 216.
https://digitalcommons.uri.edu/oa_diss/216

This Dissertation is brought to you by the University of Rhode Island. It has been accepted for inclusion in Open Access Dissertations by an authorized administrator of DigitalCommons@URI. For more information, please contact digitalcommons-group@uri.edu. For permission to reuse copyrighted content, contact the author directly.

NOVEL STRATEGIES FOR THE PURIFICATION AND
INHIBITION OF PROTEIN-TYROSINE KINASES

BY

ALEXANDER BROWN IV

A DISSERTATION SUBMITTED IN PARTIAL FULFILLMENT OF THE
REQUIREMENTS FOR THE DEGREE OF

DOCTOR OF PHILOSOPHY

IN

CELL & MOLECULAR BIOLOGY

UNIVERSITY OF RHODE ISLAND

2014

DOCTOR OF PHILOSOPHY DISSERTATION
OF
ALEXANDER BROWN IV

APPROVED:

Thesis Committee:

Major Professor Gongqin Sun

Niall G. Howlett

Keykavous Parang

Nasser H. Zawia

DEAN OF THE GRADUATE SCHOOL

UNIVERSITY OF RHODE ISLAND
2014

ABSTRACT

Protein-tyrosine kinases (PTKs) play essential roles in the cell signaling pathways of eukaryotes. However, since their discovery, PTKs have also been linked to cancer and it is now known that many of these enzymes actively promote oncogenic cell signal transduction in unregulated forms. Therefore, there has been a concerted effort on the part of researchers to identify the PTKs that potentiate such pathways, characterize their regulatory properties, and develop strategies to selectively disrupt these key elements of oncogenic signaling. Following this strategy, work described in this dissertation first focuses on the characterization of a relatively unstudied PTK, known as SRMS, which may be linked to cancer. To accomplish this, a novel strategy was developed to purify active SRMS, which can also be used to purify other PTKs for *in vitro* biochemical studies. Additionally, the purified SRMS was shown to activate upon autophosphorylation of the activation loop tyrosine, representing the first known regulatory mechanism of SRMS. The second focus of this dissertation was to develop a novel strategy for the design of selective PTK inhibitors. Using dasatinib, an established small-molecule inhibitor, a series of carboxyester-linked derivatives were synthesized and evaluated against a panel of PTKs. The biochemical data obtained presents a library of compounds with modified specificity toward individual PTKs. Thus, this strategy represents a break-through in the development of new, more selective PTK inhibitors for use as medicinal drug lead compounds.

ACKNOWLEDGMENTS

I am both proud and grateful for having Dr. Gongqin Sun as my advisor during these important years of my life. His support and encouragement has been constant and his enthusiasm, contagious. I consider the wise and objective advice he has given to me, on so many occasions, to be priceless pieces of my education and development as a scientist.

I would also like to thank the other members of my committee for their continued guidance and support: Professors Paul Cohen, Niall Howlett, Joanna Norris and, especially, Keykavous Parang. You are all very busy people and it means a great deal to me for you to give me so much of your precious time and energy.

None of this work could have been possible without the countless hours that my lab mates and collaborators have invested in our various joint endeavors. I want to thank all of these people, including Dr. Xiaofeng Lin, Dr. Kezhen Huang, Dr. David Kemble, Dr. Yuehao Wang, Dr. Wei Wei, Seetha Naramaneni, Yanping Wang, and Yixin Cui. I owe one past lab mate, Dr. Rakesh Tiwari, above all. He has worked tirelessly with me on numerous projects over these years, as part of our lab and Dr. Parang's. To you all: you are some of the hardest workers that I know, and I cannot imagine a better group of lab mates and collaborators. Thank you, my friends!

DEDICATION

This thesis dissertation is dedicated to my family and friends. I hope you will forgive me for all the good times that I've missed out on while I was too wrapped up in grad school. Regardless of how often we've gotten together, keeping you in my daily thoughts has kept me going. You have all inspired me and cared for me in so many ways... I could never have been able to pursue this dream of mine if it hadn't been for you all, thank you!

PREFACE

This dissertation was formatted in accordance with the manuscript format guidelines established by the Graduate School of the University of Rhode Island.

TABLE OF CONTENTS

ABSTRACT	ii
ACKNOWLEDGMENTS	iii
DEDICATION	iv
PREFACE	v
TABLE OF CONTENTS	vi
LIST OF TABLES	viii
LIST OF FIGURES	ix
INTRODUCTION	1
PROTEIN KINASES AND SIGNAL TRANSDUCTION	1
PROTEIN-TYROSEINE KINASES (PTKS)	5
SRMS	21
REGULATION OF PTKS	25
IN VITRO CHARACTERIZATION OF KINASES	29
PTKS AS THERAPEUTIC DRUG TARGETS	33
FOCUS OF THIS THESIS	38
WORKS CITED	40
MANUSCRIPT 1: Bacterial expression, purification and characterization of activated kinase, SRMS: a novel protocol to avoid chaperone protein co- purification	47
ABSTRACT	48
INTRODUCTION	49

MATERIALS AND METHODS	53
RESULTS AND DISCUSSION.....	61
ACKNOWLEDGMENTS.....	88
WORKS CITED	89
MANUSCRIPT 2: <i>Design, synthesis and evaluation of dasatinib-derived protein-</i>	
<i>tyrosine kinase inhibitors</i>	92
ABSTRACT	93
INTRODUCTION.....	94
RESULTS.....	102
DISCUSSION AND CONCLUSION.....	121
METHODS.....	130
WORKS CITED	135

LIST OF TABLES

TABLE	PAGE
<i>Manuscript 1: Bacterial expression, purification and characterization of activated kinase, SRMS: a novel protocol to avoid chaperone protein co-purification</i>	
Table 1. Components of the bacterial expression system for SRMS purification.	52
Table 2. Summary of SRMS purification	73
Table 3. Enzymatic activity of purified SRMS.....	77
<i>Manuscript 2: Design, synthesis and evaluation of dasatinib-derived protein-tyrosine kinase inhibitors</i>	
Table 1. Summary of inhibitor potency and selectivity	111

LIST OF FIGURES

FIGURE	PAGE
<i>Introduction</i>	
Figure 1. The conserved SH3-SH2-Kinase Domain architecture of nrPTKs.....	12
Figure 2. Non-receptor protein-tyrosine kinases.....	13
Figure 3. Sequence alignment of selected model non-receptor PTKs.....	20
Figure 4. Regulation of Src Family Kinases.....	28
<i>Manuscript 1: Bacterial expression, purification and characterization of activated kinase, SRMS: a novel protocol to avoid chaperone protein co-purification</i>	
Figure 1. Expression vector design and cloning.....	54
Figure 2. Purification of GST-SRMS using existing purification procedure.....	64
Figure 3. Optimization of washing to remove GroEL.....	67
Figure 4. Optimized SRMS purification.....	71
Figure 5. Enzyme kinetics of the purified catalytic domain of SRMS.....	75
Figure 6. SRMS autophosphorylation of the activation loop Tyr, Y395.....	81
Figure 7. Dasatinib inhibition of the active and inactive forms of SRMS.....	86
<i>Manuscript 2: Design, synthesis and evaluation of dasatinib-derived protein-tyrosine kinase inhibitors</i>	
Figure 1. Structural elements of inhibition.....	98

Figure 2. Dasatinib derivatives	100
Figure 3. Inhibitor screening results	104
Figure 4. Microsomal preparations metabolize dasatinib derivatives	115
Figure 5. Polarization binding assays using a fluorescent dasatinib derivative.....	119

INTRODUCTION

Protein kinases and signal transduction

In the last century, scientific inquiry into the biochemical and molecular mechanisms of carcinogenesis has led to many great advances in modern medicine's treatment of cancer and has profoundly enhanced our knowledge and understanding of life at the cellular level. The application of the scientific method to tumor biology was in its infancy at the beginning of the twentieth-century, a time when very little was known about cancer's causes and effective treatment strategies were not available. However, in 1911, the Rous Sarcoma Virus (RSV) was discovered to induce tumor formation in chickens by Peyton Rous.¹ Combined with the elucidation of the genetic code, Rous provided oncology researchers with a system to investigate the basic components and genetic elements of signal transduction and cellular transformation via kinases. Rous was recognized for this seminal achievement with the 1968 Nobel Prize in medicine.

Kinases as oncogenes

In the middle of the last century, oncologists began questioning the infection, or vector-driven, model of carcinogenesis and a new model began to emerge. It was postulated that the onset and progression of cancer might be controlled through the transformation of proto-oncogenes to oncogenes. Proto-oncogenes are genes that have the capacity to promote cancer development through their encoded proteins

and enzymes when they are activated by over-expression or mutation.² The precise mechanisms by which proto-oncogenes develop into oncogenes remains somewhat controversial to this day, but almost certainly involves the accumulation of harmful genetic mutations due to chance and environmental stressors.³ Following a decade of research into oncogenes, the first oncogene was discovered within the RSV genome.

This oncogene was found to be *v-src*, a viral version of a normal cellular gene of vertebrates, called *c-src*.^{4,5} This proto-oncogene is now known to be present in virtually all metazoan organisms and plays an essential role in cell signaling. Soon after its discovery, the protein product encoded by the *src* gene was found to belong to a group of enzymes called protein kinases, capable of adding a phosphate group onto the amino acid residues of cellular protein. Furthermore, Src represented a new form of kinase, distinct in its ability to phosphorylate tyrosine side-chains of its substrates, rather than serine or threonine.⁶

The isolation of the first oncogene was a long-awaited and significant milestone in its own right. However, the origins and nature of this particular oncogene, *v-src*, spawned an entire new field of research focused on understanding the role of tyrosine phosphorylation in tumor progression and normal cell physiology. The 1989 Nobel Prize in Medicine was awarded to Bishop and Varmus for their work revealing *v-src*'s cellular origins. The discovery of protein-tyrosine kinases (PTKs) like Src allowed Tony Hunter and numerous other pioneers in this new field, to discover dozens of other oncogenes and proto-oncogenes.⁷ Today, many of the known

oncogenes are kinases of some type and many others are directly influenced or closely associated with kinase phosphorylation networks.

Functional significance of kinases

Approaching the turn of the century, the basic mechanisms governing reversible protein phosphorylation by serine/threonine kinases (STKs) had also been uncovered. Work that began in the 1950's by Edmond Fischer and Edwin Krebs, who won the 1992 Nobel Prize for their contributions, was joined by new STK and PTK research that revealed the nature of protein kinases as major regulators of cellular signaling by way of protein phosphorylation in eukaryotes. Upon completion of the Human Genome Project, 473 human kinases had been discovered, largely through sequencing analysis.⁸ Protein phosphorylation by these enzymes mediates signal transduction and intracellular communication that controls cellular processes including growth, development, division, replication, transcription, differentiation, metabolism, apoptosis, homeostasis, motility, and structural rearrangements.^{9,10} Despite layers of redundancy and a system of fail-safes, disruption of these pathways is known to occur, frequently driven by oncogenic kinases, which can result in cancer and a host of other diseases.¹¹

Due to their central role in governing both normal and pathological states, protein kinases have long been considered primary targets for developing novel therapeutic drugs, particularly PTKs like Src.^{2,11,12} Great advances have been made by targeting some of the unique functional roles and structural features that distinguish

PTKs from other off-target proteins and enzymes, leading to improved drug specificity and reduced side-effects.¹³ Further advances in developing targeted therapeutics will likely rely more heavily on an enhanced understanding of the differences and commonalities that exist between individual protein kinases.

Protein-tyrosine kinases (PTKs)

All protein kinases phosphorylate proteins on a select group of amino acid side-chains: serine, threonine, or tyrosine. Each of these amino acids possesses a hydroxyl group that serves as the basis for attachment of the γ -phosphate from ATP. Although other amino acids are known to be modified by kinases, serine, threonine, and tyrosine phosphorylation are by far the most common and best understood.¹⁴

Phosphorylation is a post-translational modification, meaning that it occurs after the protein has been made. As with many other post-translational modifications, phosphorylation is a structural modification that often elicits a conformational change within the protein. In many instances, dramatic protein folding rearrangements can occur in a protein substrate, precipitating major functional and regulatory changes. In the classic example of glycogen phosphorylase, phosphorylation results in substantial rearrangements which lead to the activation of the enzyme.¹⁵ However, phosphorylation can also have an inhibitory effect on certain enzymes like isocitrate dehydrogenase and Src.^{16,17} Other enzymes, such as the protein-tyrosine kinase Src, can be regulated by more than one phosphorylation event to enable modulation of enzymatic activity via several distinct conformations.¹⁸

Importantly, protein phosphorylation is chemically reversible, but stable enough under normal physiological conditions to ensure lasting signal fidelity. To turn this signal “off”, cells employ another set of enzymes called phosphatases, which have phosphoprotein-specific catalytic ability to dephosphorylate select amino acids. There are three distinct groups of enzymes that have evolved to counter protein

kinase activity in this manner. Phosphatases like PP1, belonging to the protein phosphatase Mg^{2+} / Mn^{2+} -dependent (PPM) family, and PP2C, of the phosphoprotein phosphatase (PPP) family, are specific to serine/threonine dephosphorylation. However, the independently evolved protein-tyrosine phosphatase (PTP) family of enzymes (e.g. PTP1B) is responsible for the vast majority of phosphatase activity toward phosphotyrosine-containing proteins and peptides.¹⁹

In addition to the structure-function effects upon the substrate, phosphorylation often serves as a “tag” that can be recognized, or bound, to recruit other proteins, enzymes, and substrates of the kinase signaling pathway. To this end, many proteins and enzymes, including kinases, have evolved discrete domains that specialize in recognition of phosphorylated stretches of peptide sequence. For example, the Src Homology 2 (SH2), 14-3-3, and phosphotyrosine-binding (PTB) domains are crucial components of signaling, for their specificity toward tyrosine-phosphorylated peptides.²⁰ The ability of these domains to facilitate interaction with phosphopeptides has enabled kinases and phosphatases to develop the highly elaborate cell signaling networks that are necessary for eukaryotic organisms.^{10,21}

Eukaryotic protein kinases can be broadly grouped into two categories, STKs and PTKs, based upon their substrate preferences. Protein-tyrosine kinases differ in that they strictly phosphorylate specific tyrosine residues, not serine or threonine. Combined with the phosphotyrosine-specific binding domains and protein-tyrosine phosphatases, PTKs have evolved independently from STKs to delicately balance the kinase signaling networks of all metazoan life.^{22,23}

Defining characteristics of PTKs

PTKs diverged from STKs over half a billion years ago, just prior to the evolution of multicellularity in the metazoan lineage.²⁴ PTKs represent one of about eight uniquely metazoan families of enzymes and likely played a key role in the evolution of multicellularity by providing cells with a new signaling mechanism that would be less disruptive to the essential STK pathways, already present.²³ The protein substrates of PTKs are frequently targets for modification by STKs and other signaling enzymes, too. In this manner, serine/threonine and tyrosine phosphorylation networks, collectively known as the kinome, are an integral component of a vast network of cell signaling.

While there are no clear-cut roles or pathways that can be used to categorically distinguish the PKs from one another, there are some generalizations that can be made from the perceived influence or importance of either on certain cellular functions. STKs, like the cyclin-dependent kinases, are often thought of as the central regulators of the cell cycle, while PTKs generally appear to exert the most control over the development and differentiation of cells in response to stimuli, exemplified by the numerous growth factor receptor kinases. PTKs account for less than 1% of the total protein phosphorylation of the cell, despite having generally higher enzymatic turnover. Thus, PTKs appear to be much more tightly regulated, compared to STKs.

It has been proposed that the aromatic component of phosphotyrosine may have provided a better target for the evolution of the large number of

phosphospecific intermolecular interactions that are necessary for evolving a tightly regulated signal transduction pathway, largely mediated by SH2 domains and protein-tyrosine phosphatases (PTPs). Together, PTKs, PTPs, and SH2 domains function in concert using a 'write-read-erase' system that is both rapid and dynamic. Through this context, one can begin to understand the unique nature of PTKs as dynamic regulators of cell signaling and as obvious targets of investigation for basic and clinical research.^{8,9,13}

Structural and biochemical studies of the kinase domains of these two groups support the separate classification of STKs and PTKs.^{8,25} The catalytic loop regions of STKs frequently possess a lysine residue, such as the catalytic loop YRDLKPEN sequence found in PKA. However, PTKs share an sequence containing arginine (e.g. HRDLAARN in IRK, and numerous others) that is highly conserved. This catalytic loop, in conjunction with several other residues of the kinase catalytic domain, is largely responsible for the differences in amino acid preference observed between STKs and PTKs.²⁶ Yet, comparisons also reveal a significant level of conservation concerning the folding of the kinase domain and the molecular basis of PK catalysis within the active site.

Structure and domain architecture of PTKs

While STKs and PTKs share a great deal of homology, the relative conservation of regulatory domains/features of PTKs and the distinct pathways in which they operate suggest that PTKs merit investigation as a distinct family of enzymes,

independent from STKs. PTK catalytic domains are found to exist in about a hundred different human proteins. There are two main classes of protein-tyrosine kinases: receptor (trans-membrane) and non-receptor (cytosolic).

Receptor PTKs (RTKs) possess extracellular and trans-membrane domains, at the N-terminus, and at least one catalytic domain that resides within the cytoplasm, but in close proximity to the membrane. Currently identified, there are approximately 20 distinct families of RTKs. There are several RTKs that are prominent figures in cell signaling, including members of the fibroblast, epidermal, vascular endothelial, and insulin-like growth factor receptor (FGFR, EGFR, VEGFR, and IGFR) families. RTKs are responsible for the recognition and initiation of many different types of signaling molecules. Both large and small proteins, as well as several small molecules of native and foreign origins have been found to bind the extracellular domains of RTKs to initiate signaling cascades. Frequently, binding of the extracellular RTK substrate induces dimerization of the receptor which, in turn, promotes activation of the kinase by way of trans-phosphorylation. The active kinase will then proceed to phosphorylate one or more downstream proteins and enzymes, often amplifying the signal.

Many times, the RTKs will activate other PTKs, including non-receptor PTKs (nrPTKs) which do not exclusively associate with the cell membrane. The nrPTKs are often referred to as cytosolic, but this label fails to convey the dynamic localization patterns of these important enzymes. In fact, nrPTKs are frequently found in transit

between various cellular locations and organelles, such as the plasma membrane and the nucleus.

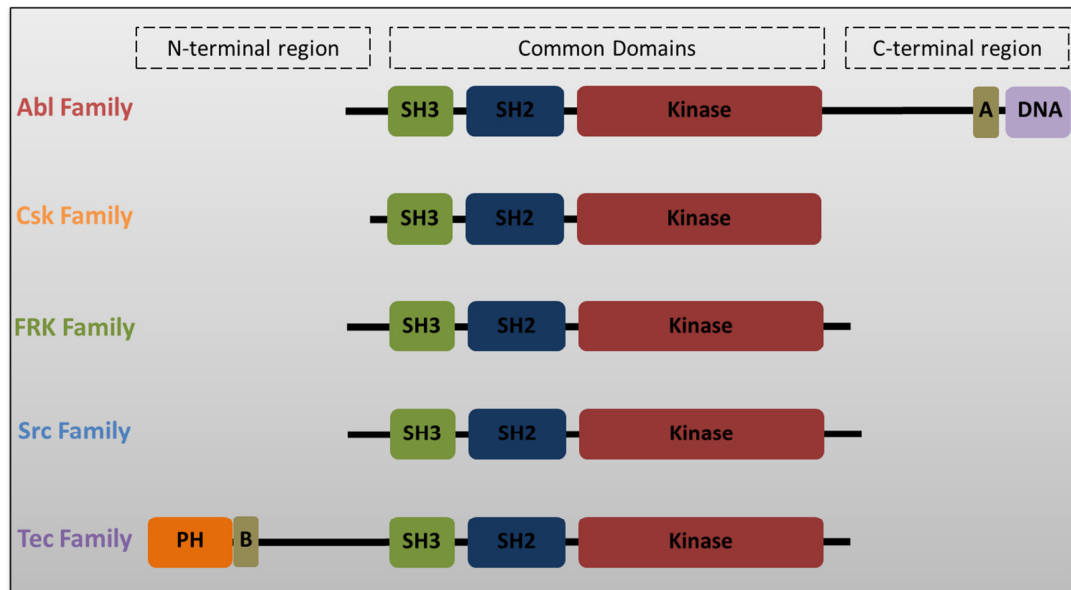
The domain architecture of nrPTKs is fairly variable, but most contain at least one Src homology 2 (SH2) domain to facilitate interaction with RTKs and other phosphorylated proteins. SH2 domains contain approximately 100 amino acids and bind to phosphorylated tyrosine containing peptides. SH2 domains are frequently responsible for localization to RTKs and other enzymes that have been activated by tyrosine phosphorylation. Aside from this prototypical function, SH2 domains also can play critical roles in the catalytic regulation of the enzymes to which they are tethered. Frequently, the SH2 domains of kinases are found just upstream of the catalytic domain.

Another prototypical nrPTKs domain is the Src homology (SH3) domain, which specializes in recognition of proline-rich peptide sequences. SH3 domains are roughly 60 amino acids long. Like SH2 domains, they can contribute greatly to localization and regulation of kinases or other SH3 domain containing proteins. In nrPTKs, the SH3 domain is positioned near the N-terminus, just before the SH2 domain. This SH3-SH2-kinase domain architecture is a common feature to the majority of nrPTKs and is exemplified by the Src, Abelson murine leukemia viral oncogene homolog 1 (Abl), C-terminal Src Kinase (Csk), Fyn related kinase (FRK), and Tec families of protein-tyrosine kinases.

In addition to the aforementioned SH3 and SH2 domains, over two dozen different types of accessory protein sequences and domains can be found alongside

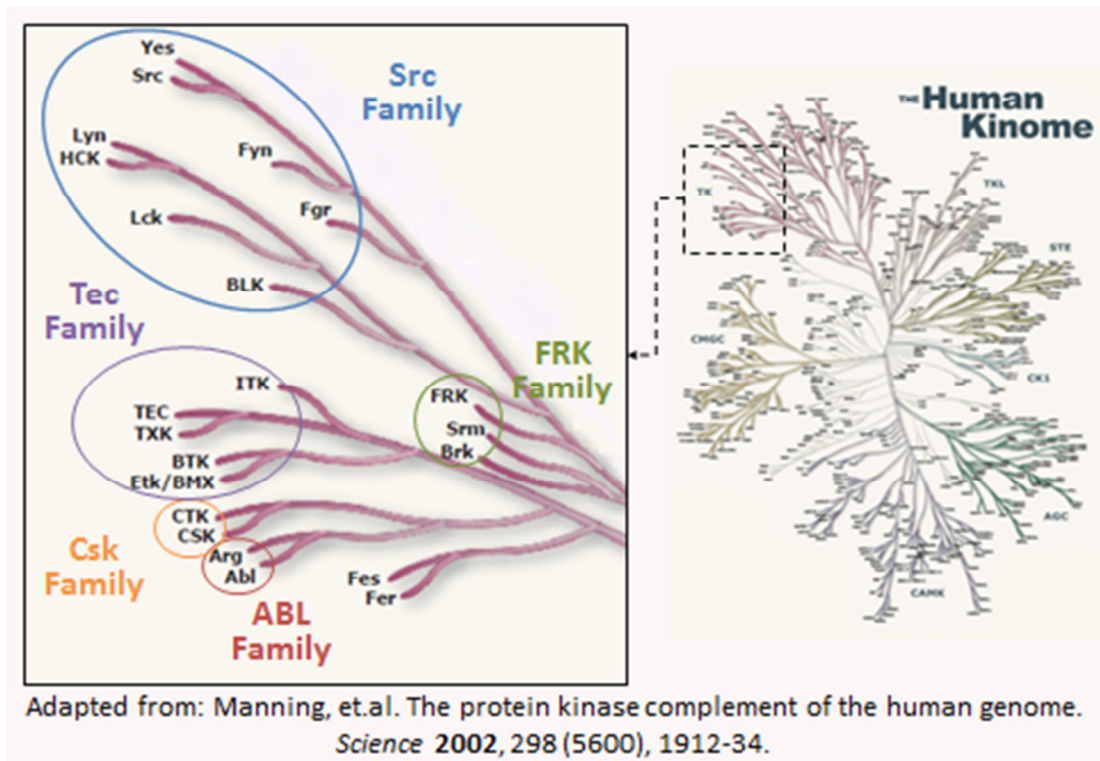
PTK catalytic domains, at either the N- or C-terminal regions of the kinases. Many of these domains are found to contribute to the regulation of the kinase domain, by way of intramolecular and intermolecular interactions. Such interactions modulate the kinase activity by stabilizing or destabilizing the active and inactive conformations of the catalytic domain. Furthermore, accessory protein domains frequently determine or influence sub-cellular localization and recruitment of PTK substrates through direct and indirect molecular complexes.

Figure 1. The Conserved SH3-SH2-Kinase Domain Architecture of nrPTKs



A, Actin binding domain; **B**, Btk homology domain; **Kinase**, PTK catalytic domain; **PH**, Pleckstrin homology domain; **SH2**, Src homology 2 domain; **SH3**, Src homology 3 domain

Figure 2. Non-receptor protein-tyrosine kinases



Model kinases of interest

The large number and diversity of PTKs, including non-receptor PTKs, presents a daunting challenge to researchers attempting to understand the signaling dynamics of cells. In order to narrow the focus of research, PTKs have been subdivided and grouped according to their structural similarities. Besides possessing a high degree of sequence homology, there is a clear pattern of conservation regarding accessory domains and other known regulatory features within each of these families. The observed characteristics of a single, model kinase can be used to infer similar functionality to other related enzymes that share the necessary structural components.

In this manner, implicit models can be created to help piece together a view of the larger signaling dynamic of the cell and provide the insight necessary for future investigation and further refinement of our understanding. The Src, Abl, Csk, FRK, and Tec enzymes often serve as model kinases, representing their respective family member nrPTKs. Studying the structural and functional differences between these kinases has proven to be instrumental in understanding how nrPTKs help to govern cell signaling.

Src was the first PTK discovered and, therefore, rapidly became one of the best studied enzymes. Src and other Src family kinases (SFKs) are best known as major components to many growth factor signaling pathways, often directly interacting with growth factor receptors. Through various receptors, SFKs help to regulate growth, differentiation, migration, survival, and numerous other processes

in tissues throughout the body. Abnormally elevated SFK activity levels are closely associated with oncogenesis in humans, particularly in certain types of colon cancers, melanoma, leukemia, and lymphoma.

Similarly, Abl family kinases (AFKs) are best known for their potential to cause cancer. Philadelphia chromosome positive ALL and CML is a direct result of oncogenic Abl. However, like Src and other proto-oncogenic PTKs, Abl also contributes to normal cell signaling pathways such as growth, survival, and the DNA-damage response.²⁷ Abl family kinases are most notably distinct from SFKs due to their N-terminal Tec homology (TH) domain and Pleckstrin homology (PH) domain and large C-terminal region which contain numerous accessory domains governing kinase localization and function. Within the C-terminal region, Abl contains three nuclear localization signals and a nuclear export signal, which is suggestive of the tight, highly dynamic regulation of this PTK.²⁷

Aside from their roles in malignancy, PTKs can also play major parts in tumor suppression. Csk and its relatives are known tumor suppressors. These PTKs phosphorylate other kinases, particularly the SFKs, rendering them inactive. In fact, the Csk family of enzymes appears to have evolved almost exclusively to negatively regulate SFKs, keeping their signals in check and preventing oncogenic signaling. Inactivation of SFKs by Csk is perhaps the best understood mechanism of nrPTK regulation. Study of this interaction has greatly enhanced understanding of PTK substrate specificity.

After the SFKs, the Tec family of kinases (TFKs) is the largest group of nrPTKs. Expressed primarily in hematopoietic cells, such as T cells, TFKs play vital roles in the signaling of the immune response and lymphocyte development. This kinase family appears uniquely regulated and contains various N-terminal domains such as proline-rich regions, TH domain, and/or PH domains. Operating downstream of antigen receptors, Tec family kinases often become activated through SFK-mediated tyrosine phosphorylation.²⁸ Aside from normal cellular function, the role of these kinases in human disease is much less clear at this time.

The last of the nrPTK groupings is the FRK family kinases (FFKs). Little is known about these kinases, which have only recently been revealed to be distinct from SFKs. While there does appear to be some overlapping substrate specificity with SFKs, several novel interactions have also been reported. Importantly, FFKs appear to possess the capacity to operate as both tumor suppressors and oncogenes, depending on the cellular context.²⁹ However, the mechanisms by which FFKs maintain such a dynamic is currently unknown. The FFKs are discussed in further detail later in this review.

PTKs share a common mechanism of catalysis, yet each of these nrPTK families has evolved to perform unique functions within the cellular environment. Many kinases are co-expressed within a given cell and yet each achieves very different patterns of phosphorylation. This can only be possible if the regulation of their enzymatic capabilities is finely tuned to suit the evolved genetic program. How each of these related kinase families co-evolved to maintain such a dynamic is not

completely understood. Therefore, much research has focused on identifying the unknown features that are responsible for each kinase's unique activity profile.

PTK enzyme catalysis

In order to understand the differences between PTKs, it is essential to identify commonalities that may exist. Structural and biochemical studies of many kinases have revealed a great deal about the essential catalytic ability of these enzymes. By comparing the relative catalytic abilities and structural differences between kinase families, several key components of PTK regulation are now well understood.

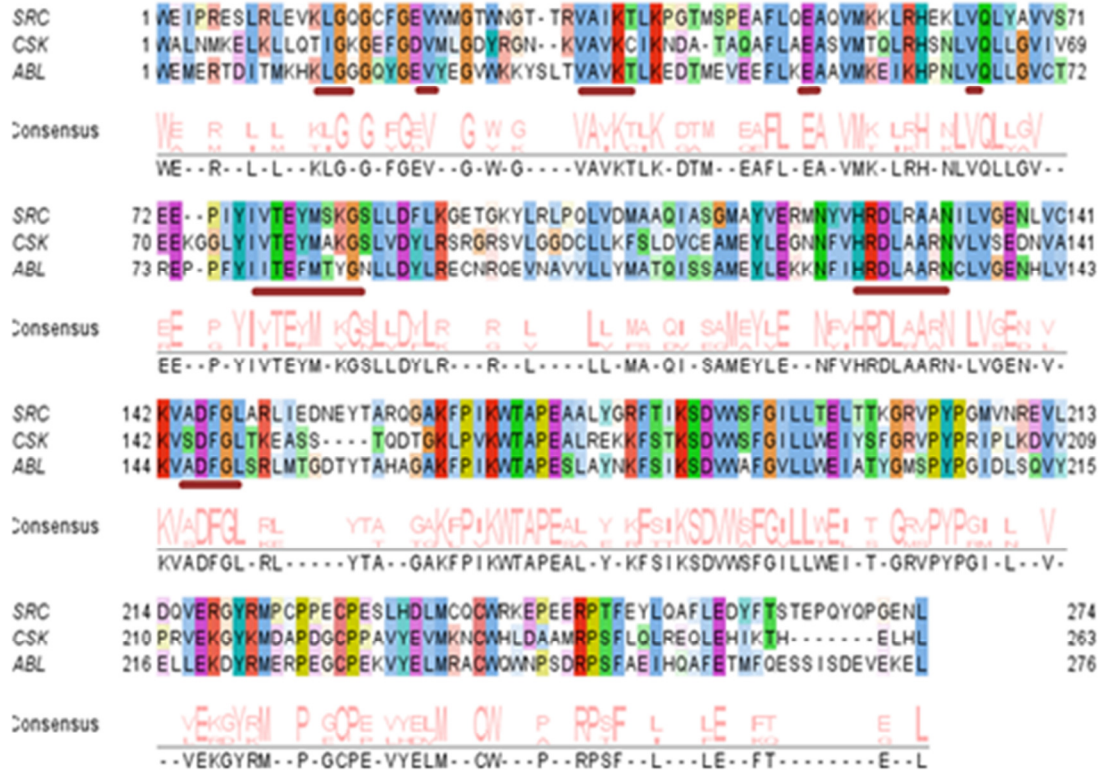
PTK catalytic domains consist of two distinct lobes, hinged together to form the catalytic cleft.³⁰ Most of the N-terminal residues of the catalytic domain form the ATP-binding lobe, while many of the C-terminal residues are contained within the lobe commonly referred to as the substrate binding lobe.³⁰ Each of these subdomains is a monomer, however, since both domains play crucial roles in binding ATP and other substrates of the kinase. In the active conformation(s), the PTK must simultaneously bind both of its substrates, peptide and ATP, within the active site.³¹

As ATP and the tyrosine containing peptide each bind, ATP hydrolysis and transfer of the γ -phosphate occur independent of an intermediate step. Catalysis is greatly enhanced in the presence of normal physiological concentrations of several divalent metal cations, frequently Mn^{2+} or Mg^{2+} , which can bind dynamically to the catalytic cleft of the enzyme.³² While PTKs accomplish substrate phosphorylation with a wide range of efficiency, their catalytic mechanisms are virtually identical. This is reflected quite clearly by the high degree of conservation observed within multiple sequence alignments of the PTK catalytic domains (Figure 3), particularly within the active site.

The specific amino acids that surround the tyrosine residue of the substrate are known to have dramatic effects on overall catalytic efficiency. However, there is no clear pattern of preference that is shared between all PTKs, with regard to the specific sequence of amino acids adjacent to the target tyrosine of known substrates. This means that a small tyrosine containing peptide that is a great substrate for one PTK will not necessarily be phosphorylated by a different PTK, even if both enzymes are determined to be equally active toward a common substrate. For example, Src and Csk are both able to phosphorylate the generic substrate PolyE₄Y quite well, yet Csk is unable to phosphorylate known Src substrates such as Cortactin. Likewise, Src shows no significant activity toward its own C-terminal tail tyrosine, a known substrate for Csk.³³

In addition to the variability of efficiency stemming from local sequence preferences, enhanced catalytic efficiency can also be achieved through more distally located interactions. In such cases, the local sequence appears to play only a minor or secondary role as other, more remote docking sites facilitate interaction, or substrate recognition. One such case is the docking interaction of Src to Csk. In order for Csk to phosphorylate the C-terminal tail tyrosine, to inactivate the enzyme, a stretch of amino acids from Csk's substrate binding lobe, RSRGRS, is an essential part of the recognition of Src. This region, well outside the catalytic cleft, is necessary to achieve phosphorylation and inactivation of Src via Csk.³³

Figure 3. Sequence alignment of selected model nrPTKs.



Surface residues of the ATP-binding pocket are underlined in red

SRMS

As more is uncovered about each kinase, our model of the elaborate network of PTK signaling within the cell is improved. When researchers began focusing more closely upon the distinct members of the Src family kinases, it became apparent that several of these kinases were relative outliers in terms of their genetic, structural, and functional differences. These outliers were re-classified into a new family of nrPTKs and the true nature of these enzymes continues to be a focus of research, at present. The human members of the FRK family of non-receptor PTKs (FFKs) initially appeared to share identical accessory domain architecture with SFKs. However, closer inspection has revealed many elements that are crucial to the functional regulation of SFKs appear to be absent or markedly distinct within the FFKs.

FRK family kinases

FRK, also known as RAK, has been found in human liver, kidney, mammary, and epithelial tissues and appears to play roles in cell growth, differentiation, apoptosis, and proliferation.²⁹ Like all FFKs, FRK does not appear to localize to the cell membrane in the same manner as SFKs, due to a lack of a functional N-terminal myristoylation domain. However, FRK does contain a functional nuclear localization signal within its SH2 domain.³⁴ The enzymatic regulation of FRK is thought to resemble that of SFKs, due to the presence of conserved tyrosine residues within both the activation loop and C-terminal tail regions.

Found on chromosome 6 q21-22.3, FRK is reported to be amplified in several colon cancers³⁴ and many mammary tumors³⁵, suggesting its potential as an oncogene. In contrast, this region is also frequently deleted in several breast cancers³⁶ and appears to activate PTEN, a known tumor suppressor.²⁹ PTEN has been found to be a direct substrate of FRK, and phosphorylation of PTEN by FRK prevents PTEN degradation.³⁷ PTEN, in turn, inhibits the function of AKT, and therefore, the phosphoinositol-3-kinase/AKT growth, proliferation, survival, and metabolism pathways.

Brk is also known to play an inhibitory role in this pathway, through direct interaction with AKT.³⁸ Brk, sometimes also referred to as PTK6 or PTK70, is the second member of the loosely-related FFKs. Brk shares 44% amino acid identity with FRK.²⁹ For comparison, Src and Abl share 41% identity, despite being grouped into different families.²⁷ Brk also appears to share the components necessary for Src-like regulation. Brk is located on chromosome 20 q13.3-13.4 of humans and has been implicated in apoptosis, differentiation, and cell migration.²⁹ Primarily expressed in differentiating intestine and skin cells, Brk is also amplified in several breast cancers, with and without the neighboring HER2 oncogene.³⁹

Thus, like FRK, Brk has been found to both promote and suppress the oncogenic potential of specific tissues. Together, this suggests that the FRK family kinases are dynamically regulated in a tissue and context-specific manner. FRK and Brk appear to share some functional overlap with each other, as demonstrated by their common influence on the AKT signaling pathway. However, a great deal is still

unknown of these two FRK members. SRMS is the last human PTK member of the FRK family, and even less is known of this enzyme.

SRMS is located approximately 1 kb downstream from Brk, likely arising from an ancient duplication event. Additionally, the exon structure of all three human FRKs is nearly identical. Despite these similarities, the primary structure of SRMS appears to be quite dissimilar in several important ways. Specifically, sequence analysis indicates that SRMS lacks a C-terminal tail tyrosine and it is unclear whether its SH3 domain is functional. Beyond some limited expression data and brief mentions within the context of other studies, very little is known about SRMS.

Significance of SRMS

Within the understudied FRK family of nrPTKs, SRMS is the least well characterized. This enzyme was discovered from various tissues of mice in 1994, and has since been found to be expressed in rats and humans, as well.^{8,40} Beyond its discovery, no published data currently exists to describe the purification, potential function, or regulation of this enzyme. However, metadata available from high-throughput assays of normal and experimental tissue samples supports the ubiquitous pattern of expression described in these early reports.

The wild-type catalytic domain of SRMS has been purified from insect cells and is commercially available through several companies. Several reports have utilized such sources of SRMS, but due to low intrinsic activity toward the chosen substrates, it is unclear whether this form of SRMS is suitable for in depth studies.

Without any viable means of generating the necessary constructs for full *in vitro* biochemical study, SRMS has gone virtually unstudied. Yet, each of its most closely related kinases have been implicated in major signaling pathways of cancer cells and tissues. Additionally, SRMS offers a unique chance to study regulatory mechanisms of kinases because it does not appear to contain the key regulatory structural features found in many model kinases.

Regulation of PTKs

Although the primary function of PTKs is to propagate cellular signals via tyrosine phosphorylation, these enzymes are often substrates, themselves, of upstream PTKs. Many tyrosine kinases are known to be regulated by numerous post-translational modifications, particularly via tyrosine phosphorylation. In fact, phosphorylation by other kinases and dephosphorylation by phosphatases appears to be a primary regulatory mechanism of PTK activity. In some cases, patterns of phosphorylation appear to have a greater impact on overall kinase activity than even large-scale changes in expression could produce. Thus, there are a few conserved mechanisms of PTK regulation by phosphorylation that must be considered.

Activation of PTKs by autophosphorylation

Most PTKs contain a flexible peptide loop region within the substrate binding lobe that harbors a tyrosine residue. This amino acid, upon phosphorylation, often activates the kinase by stabilizing the active conformation. Therefore, this region of the catalytic domain has come to be known as the activation loop. Many kinases possess the ability to phosphorylate this position in *trans* fashion, and is referred to as autophosphorylation. Many PTKs that are regulated by autophosphorylation, including the Src family kinases, have been shown to be activated many fold following phosphorylation, with profound cellular consequences.

Besides Src and its closest relatives, Abl is also capable of autophosphorylation within the activation loop, leading to activation *in vitro*.⁴¹ Thus,

phosphorylation of the activation loop serves as an important molecular marker of potential PTK activity for both Src and Abl. Some kinases are unable to autophosphorylate their activation loop tyrosine. For example, activation loop phosphorylation increases Tec family kinase activity. However, these kinases do not appear to self-phosphorylate.²⁸ Other PTKs like Csk contain no activation loop tyrosine residue at all. Thus, the role that activation loop phosphorylation or autophosphorylation has in PTK regulation appears to be a major mechanism of regulation that has been differentially conserved by non-receptor PTKs.

Inactivation of PTKs

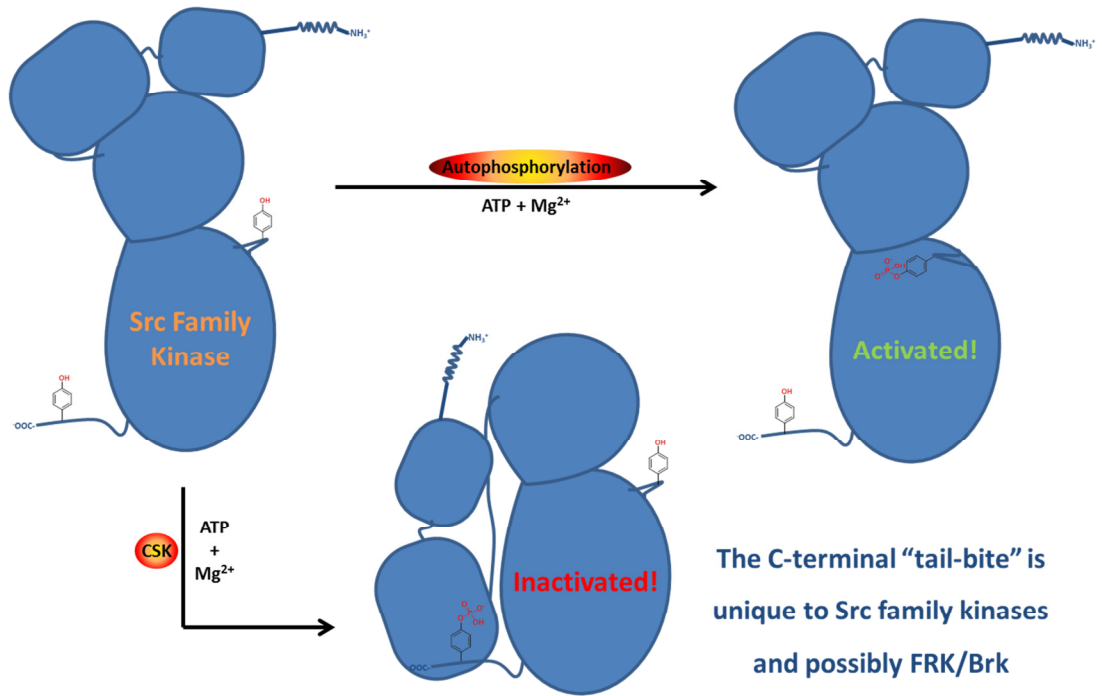
Phosphorylation is also known to inactivate kinases. In the classic example, the Src family kinases may be phosphorylated at an alternative regulatory position on a short, conserved peptide “tail” that contains a tyrosine residue, just following the C-terminal portion of the catalytic domain. This C-terminal tail is exclusively phosphorylated by Csk.¹⁷ Upon phosphorylation of the tail tyrosine by Csk, Src undergoes a dramatic conformational rearrangement, leading to an inhibited conformation. In crystal structures of this inactive form of the kinase, the SH2 domain of Src is bound to the C-terminal tail phosphotyrosine in what is known as the “tail-bite” conformation.³⁰

The phosphorylation of the activation loop and C-terminal tail are two opposing mechanisms and are perhaps the two best understood modes of nrPTK regulation. Although many PTKs possess an activation loop tyrosine, and therefore

the capacity to be regulated by autophosphorylation, relatively few mechanisms of inactivation have been confirmed for PTKs beyond the Src family tail-bite conformation. However, C-terminal tail phosphorylation may not be required for some kinases to achieve similar inhibited forms.

In the case of Abl, found in PDB entry 1OPK, the auto-inhibited enzyme reveals a conformation that is surprisingly similar to Src's tail-bite form.⁴² Even though Abl lacks a C-terminal tail tyrosine, the myristoylation domain of its N-terminus appears to facilitate the necessary interactions between the SH2 and catalytic domains to inhibit the enzyme.²⁷ Additional modes of negative regulation have been proposed for other families of nrPTKs that lack a conserved C-terminal tyrosine, as well.

Figure 4. Regulation of Src Family Kinases



***In vitro* characterization of kinases**

Much of what is known today of the function and regulation of kinases has been pieced together from the careful analysis of *in vitro* biochemical data. Purifying proteins and enzymes from *in vivo* tissue samples is frequently possible, but this approach is often quite limiting to researchers. Yields obtained from living or cultured sources are typically low and mutational analysis is difficult. Therefore, recombinant protein expression systems are often favored for obtaining and purifying sufficient amounts of active enzyme for use in biochemical assays. However, purification of active kinases from recombinant expression and purification strategies has proven relatively difficult, historically.

Systems of expression and purification

PTKs are most commonly expressed within two different hosts for high yield production of active, recombinant enzyme: insect cells and *E. coli*. Insect cells generally are able to produce the highest yields, yet growth time and cost are two major downsides for many studies. This system is expensive and particularly difficult to rapidly generate many different constructs of a single enzyme for mutational analysis. *E. coli*, however, is both rapid and inexpensive.⁴³ Moreover, numerous advancements have been made toward improving the overall yield of enzyme produced from bacterial expression, through optimization of growth media.⁴⁴ Thus, heterologous expression of kinases within *E. coli* is generally a preferred means of producing active enzyme for *in vitro* characterization.⁴⁵ Despite the numerous

advantages offered from recombinant expression systems, there are several potential pitfalls that may prevent the purification of active kinase from these systems.

Major obstacles to expression and purification of PTKs from E. coli

Prokaryotes, such as *E. coli*, have not evolved to tolerate high levels of tyrosine phosphorylation. Therefore, high level expression of kinases frequently becomes toxic to the bacteria and greatly diminishes overall yield and/or reliability of the enzyme obtained. In such cases, several strategies have been employed to successfully counteract the toxicity of recombinant PTK expression: reducing “leaky” expression and co-expression alongside a recombinant protein-tyrosine phosphatase (PTP). Many strategies exist to reduce leaky expression and improve inducible promoter control,⁴⁶ but many appear insufficient for recombinant expression of select PTKs. However, co-expression of PTKs alongside PTPs, such as PTP1b, has alleviated toxicity of PTKs in a number of bacterial systems.^{45,47,48} Phosphatase co-expression systems have been successfully employed to produce important Src and Tec family kinases, as well as several receptor PTKs of clinical interest.

Besides toxicity concerns, proper protein folding and solubility are also particularly difficult to achieve with some PTKs expressed in bacterial systems. Solving such problems in expression and purification is perhaps the largest, most difficult task for kinase researchers, currently. Frequently, PTK folding and solubility can be improved by expressing these enzymes as fusion proteins to common affinity

chromatography tags, such as glutathione S-transferase (GST) and maltose binding protein (MBP).⁴⁹ Also, due to the relatively rare use of certain codons within prokaryotes, codon optimization and/or co-expression of genes that elevate levels of specific amino-acyl tRNAs have also proven quite effective to improve solubility of heterologous proteins.⁵⁰ Several *E. coli* strains have been developed to circumvent rare codon usage and these commercially available expression hosts have proven quite successful.

Despite affinity tag and codon usage optimization, many PTKs remain difficult to purify in sufficient quantities due to improper folding and/or poor solubility. To address this issue, several *E. coli* expression systems have been supplemented with additional genes to produce various chaperone proteins. These proteins serve to guide protein folding and re-folding and are frequently used for expression of PTKs and many non-PTK enzymes, as well.^{51,52} The GroES and GroEL proteins that make up the GroESL chaperone complex are among the most frequently used in the recombinant expression of PTKs.

GroEL is a member of the Hsp60 family of protein chaperones, found in eukaryotic mitochondria and prokaryotes such as *E. coli*.⁵¹ GroEL may independently aid in the folding and solubility of proteins, but commonly associates with the much smaller GroES. GroEL associates independently into a grand molecular cylinder, consisting of two heptameric GroEL rings. Seven GroES members also self-assemble to form molecular “caps” to the GroEL cylinder, trapping the improperly folded protein within, and ATP hydrolysis serves to power protein re-folding by the

macromolecular assembly.⁵³ A major drawback to GroESL overexpression systems is the tendency of GroEL to co-elute with recombinant protein of interest, requiring further purification steps.^{48,54} Despite this potential complication, GroESL and other chaperones have proven quite successful in obtaining soluble, active kinases.

Each of these strategies to alleviate toxicity and improve solubility and folding of PTKs in recombinant expression systems has proven successful in producing high yields of active kinase. Often, several or all of the discussed strategies are employed to achieve adequate expression and purification of nrPTKs. Despite all the PTKs purified successfully, no universal expression system currently exists. Since researching the biochemical nature of a given kinase is frequently plagued by one or more of these issues, there remains great interest in optimizing existing strategies and developing new methods for the expression and purification of PTKs.

PTKs as therapeutic drug targets

Inactivation of kinases is an important objective for the treatment of many diseases. Under-regulated or overly stimulated kinase activity can lead to disastrous consequences for the affected cell, tissue, and the entire body. In the case of many cancers, in particular, such kinases cause or drive the cell changes necessary for proliferation and metastasis. Therefore, for over two decades, a great deal of interest has been paid to the development of safe, effective kinase inhibitors for the treatment of various afflictions. However, often times it is unclear which kinases to target to achieve effective therapeutic strategies.

In addition to those previously discovered kinases, the completion of the human genome project allowed for the identification and classification of all PTKs within the human kinome. Through analysis of the structure and expression, these PTKs have been grouped and labeled as members of various families. However, it may be important to note that such distinctions are frequently made without the proper empirical data to conclusively differentiate the cellular function and/or regulation of separate PTK families. Thus, identifying the PTKs that directly influence a given pathology can become quite difficult, and the literature is full of evidence that is seemingly contradictory, greatly confounding the efforts to choose an appropriate PTK target for design of novel therapeutics.

Another hurdle to the development of kinase inhibitors has been generating proper specificity toward the errant kinase, or kinases, in order to refrain from damaging normal processes of the target tissues. Within the last ten years, major

breakthroughs have enabled the therapeutic targeting of PTKs and, in some cases, eliminated the need for highly toxic and non-specific radiation and chemotherapeutic treatments. By harnessing the power of small molecule PTK inhibitors, anticancer treatments have made significant progress in targeting PTKs that drive cancer.

Small molecule PTK inhibitors

In some acute lymphoblastic and chronic myeloid leukemia patients, a specific genetic defect called the Philadelphia chromosome (Ph^+) results in the expression of an unregulated form of the PTK, Abl. This errant kinase is actually a fusion protein which consists of a truncated form of the BCR protein that replaces portions of the N-terminal regulatory domain of the Abl kinase (BCR-Abl). Without this region, autoinhibition of Abl is greatly impaired, leading to the reprogramming of the cell signaling network and, ultimately, leukemia. Thus, BCR-Abl represents one of the best, clear-cut examples of a PTK drug target.

In 2004, Bristol-Myers Squibb announced the discovery of Gleevec, or imatinib, as the first small molecule compound to effectively target BCR-Abl and treat Ph^+ patients. Prior to the introduction of imatinib, Ph^+ patients suffered intolerable treatment regimens and incredibly high mortality rates. Imatinib and several other drugs with similar mechanisms of action have now been approved for various pathologies, greatly enhancing patient outcomes through targeted disruption of PTKs. Guided by the successes of imatinib, the investigation of new and improved PTK inhibitors has been and continues to be of great interest.

Generating PTK specificity

The structure of imatinib and the other small molecule PTK inhibitors are often quite dissimilar, yet each inhibits BCR-Abl by binding to the ATP-binding cleft of the kinase. This high affinity interaction disrupts the recruitment of substrate and/or reduces catalytic activity. The precise region of the catalytic cleft that each inhibitor may occupy is somewhat variable, from compound to compound. However, within this small cleft, there are a limited number of residues and/or motifs that may significantly contribute toward generating the type of high affinity interaction that a PTK inhibitor requires. Because of this, a simple mutation in BCR-Abl can result in resistance to multiple inhibitors.¹²

Additionally, since the active sites of many kinases are generally well conserved, it is often difficult to generate novel compounds that exclusively disrupt the target kinase. For example, while imatinib can inhibit Abl at sub-micromolar concentrations, it has also been demonstrated that similar concentrations can disrupt off-target kinases, such as KIT, Lck, and PDGFR.^{55,56} Later generation drugs targeting BCR-Abl, such as dasatinib (Sprycel) and nilotinib (Tasigna), also inhibit several known off-target kinases. In addition to these kinases, it has been proposed that any of the over 2,000 other nucleotide-dependent enzymes that are found in humans could be potential targets, due to similarities they share with the active sites of PTKs.¹² Through examination of primary sequence alignments that compare various nrPTKs, it is clear that those regions responsible for interacting with most of the approved and investigational drugs are among the better conserved portions of

kinases. However, there are other regions that show great variation and may provide better targets for new drugs aimed to improve the specificity of PTK inhibition.

Drug resistance and toxicity

It is widely believed that most patients undergoing treatment with kinase inhibitors will eventually develop resistance. Drug resistance arises from several possible events that commonly occur during the progression of tumorigenesis, because cancerous cells are frequently in a state of constant genetic flux. Deletions, amplifications, translocations, and mutations are not only causes of cancer, but also drivers of its progression and a means to acquire drug resistance. Many mutations have been found in cancer cells that disrupt inhibitor binding. Because of this, second generation kinase inhibitors have been developed, such as dasatinib, which are able to bind despite many of these common mutations.⁵⁷

However, even dasatinib, one of the best second generation drugs, fails eventually due to the accumulation of certain additional mutations. For example, the mutation of amino acids at positions homologous to a threonine in Abl (T315I), KIT (T670I), and EGFR (T790M), all confer clinical resistance to imatinib. This residue (known as the gatekeeper) is one of a handful of mutations that can destroy the effectiveness of dasatinib and all other second-generation kinase inhibitors as well.⁵⁶

Examination of the crystal structures of kinases, in complex with these compounds, reveals that the gatekeeper residue resides in the ATP-binding cleft of the kinases and forms a hydrogen bond with each of the inhibitors. Without the

gatekeeper-inhibitor interaction, these mutant kinases are much less energetically suited to bind the therapeutic compounds and often require concentrations of several orders of magnitude greater to achieve inhibition. Often, these dosages prove to be toxic to patients and would result in significant side effects or even death.

The problem of toxicity may seem to exacerbate the issues of resistance; however, it is important to note that toxicity can contribute to the development of drug resistance, in the first place. Imatinib was originally reported as an inhibitor of the Abl kinase domain, but has since been confirmed to target numerous other kinases at clinical, and even subclinical, concentrations. No kinase inhibitor has been experimentally shown to target a single, clinically relevant kinase without simultaneously inhibiting other “off-target” kinases. While kinase inhibitors have undoubtedly proven to be a major advancement in the specificity of chemotherapy, clinical doses must still be tempered to alleviate the toxic side effects that are caused, in part, by the inhibitors’ lack of specificity. With such lower doses, there is a greater risk of the cancer progressing and developing resistance before complete eradication of the diseased tissues’ cells.¹² Therefore, there is currently great interest in the development of novel compounds with enhanced specificity toward PTKs to help alleviate the major problems of toxicity and resistance.

Focus of this thesis

The experimental data, results, and discussion of work derived from this thesis focuses on two distinct projects, yet each are aimed at identifying specific elements of PTKs that may serve to regulate the enzymatic activity of these highly important and influential enzymes. The first of these projects centers on the hitherto understudied kinase, SRMS, and should provide the first major clues to its function regulation and role within the kinome. The second project involves several different model PTKs and explores the potential to generate improved kinase specificity from a novel approach to small molecule PTK inhibitor design.

Investigating SRMS as a unique PTK model

Upon its discovery in 1994, the SRMS kinase was erroneously labeled as a Src family member PTK. Twenty years later, there are few studies that report any empirical data on the enzyme's attributes or provide any evidence of a cellular function. Thus, the work described in this thesis began by developing an affordable, adaptable, and reproducible system of expression and purification of the active enzyme. The purification techniques developed for the isolation of SRMS are also broadly applicable to other PTKs of clinical interest, representing a significant technical achievement. Specifically, the developed methods described provide a novel way to remove a common contaminant (GroEL), thereby improving purification of PTK samples. Based upon this work, the project was then able to reveal the first

major regulatory mechanism known to govern this enzyme's activity and highlight several other potential avenues for further investigation of this understudied PTK.

Developing novel PTK inhibitors

The second aim of this thesis explores a novel strategy for augmenting existing small molecule inhibitors with a small library of select compounds. The goal of this strategy is to extend the binding pocket of the inhibitors, in hopes of reaching highly variable regions outside of the conserved ATP-binding cleft, thereby generating enhanced specificity. The synthesis strategy that was employed in this study was based on work performed by several other groups. In their studies, existing inhibitors were used for the attachment of chemical adducts that were presumed to protrude from the ATP-binding pocket. While the compounds derived by these groups were used for affinity capture purposes, the focus of the current study was to ascertain the feasibility of adapting this method to drug discovery, using the high affinity inhibitor dasatinib as a model.

Works Cited

- 1 Rous, P. A Transmissible Avian Neoplasm. (Sarcoma of the Common Fowl.). *The Journal of experimental medicine* **12**, 696-705 (1910).
- 2 Huebner, R. J. & Todaro, G. J. Oncogenes of RNA tumor viruses as determinants of cancer. *Proc Natl Acad Sci U S A* **64**, 1087-1094 (1969).
- 3 Varmus, H. The new era in cancer research. *Science* **312**, 1162-1165, doi:10.1126/science.1126758 (2006).
- 4 Oppermann, H., Levinson, A. D., Varmus, H. E., Levintow, L. & Bishop, J. M. Uninfected vertebrate cells contain a protein that is closely related to the product of the avian sarcoma virus transforming gene (src). *Proc Natl Acad Sci U S A* **76**, 1804-1808 (1979).
- 5 Hanafusa, H., Halpern, C. C., Buchhagen, D. L. & Kawai, S. Recovery of avian sarcoma virus from tumors induced by transformation-defective mutants. *The Journal of experimental medicine* **146**, 1735-1747 (1977).
- 6 Hunter, T. & Sefton, B. M. Transforming gene product of Rous sarcoma virus phosphorylates tyrosine. *Proc Natl Acad Sci U S A* **77**, 1311-1315 (1980).
- 7 Croce, C. M. Oncogenes and cancer. *The New England journal of medicine* **358**, 502-511, doi:10.1056/NEJMra072367 (2008).
- 8 Manning, G., Whyte, D. B., Martinez, R., Hunter, T. & Sudarsanam, S. The protein kinase complement of the human genome. *Science* **298**, 1912-1934, doi:10.1126/science.1075762 (2002).
- 9 Hunter, T. Tyrosine phosphorylation: thirty years and counting. *Current opinion in cell biology* **21**, 140-146, doi:10.1016/j.ceb.2009.01.028 (2009).

- 10 Lemmon, M. A. & Schlessinger, J. Cell signaling by receptor tyrosine kinases. *Cell* **141**, 1117-1134, doi:10.1016/j.cell.2010.06.011 (2010).
- 11 Cohen, P. Protein kinases--the major drug targets of the twenty-first century? *Nature reviews. Drug discovery* **1**, 309-315, doi:10.1038/nrd773 (2002).
- 12 Zhang, J., Yang, P. L. & Gray, N. S. Targeting cancer with small molecule kinase inhibitors. *Nature Reviews Cancer* **9**, 28-39 (2009).
- 13 Tarrant, M. K. & Cole, P. A. The chemical biology of protein phosphorylation. *Annual review of biochemistry* **78**, 797-825, doi:10.1146/annurev.biochem.78.070907.103047 (2009).
- 14 Ubersax, J. A. & Ferrell, J. E., Jr. Mechanisms of specificity in protein phosphorylation. *Nature reviews. Molecular cell biology* **8**, 530-541, doi:10.1038/nrm2203 (2007).
- 15 Johnson, L. N. & Barford, D. The effects of phosphorylation on the structure and function of proteins. *Annual review of biophysics and biomolecular structure* **22**, 199-232, doi:10.1146/annurev.bb.22.060193.001215 (1993).
- 16 Hurley, J. H., Dean, A. M., Thorsness, P. E., Koshland, D. E., Jr. & Stroud, R. M. Regulation of isocitrate dehydrogenase by phosphorylation involves no long-range conformational change in the free enzyme. *J Biol Chem* **265**, 3599-3602 (1990).
- 17 Okada, M. & Nakagawa, H. A protein tyrosine kinase involved in regulation of pp60c-src function. *J Biol Chem* **264**, 20886-20893 (1989).
- 18 Roskoski, R., Jr. Src kinase regulation by phosphorylation and dephosphorylation. *Biochem Biophys Res Commun* **331**, 1-14, doi:10.1016/j.bbrc.2005.03.012 (2005).
- 19 Barford, D., Das, A. K. & Egloff, M. P. The structure and mechanism of protein phosphatases: insights into catalysis and regulation. *Annual review of biophysics and biomolecular structure* **27**, 133-164, doi:10.1146/annurev.biophys.27.1.133 (1998).

- 20 Pawson, T. & Scott, J. D. Signaling through scaffold, anchoring, and adaptor proteins. *Science* **278**, 2075-2080 (1997).
- 21 Kholodenko, B. N. Cell-signalling dynamics in time and space. *Nature reviews. Molecular cell biology* **7**, 165-176, doi:10.1038/nrm1838 (2006).
- 22 Hanks, S. K. & Hunter, T. Protein kinases 6. The eukaryotic protein kinase superfamily: kinase (catalytic) domain structure and classification. *FASEB journal : official publication of the Federation of American Societies for Experimental Biology* **9**, 576-596 (1995).
- 23 Lim, W. A. & Pawson, T. Phosphotyrosine signaling: evolving a new cellular communication system. *Cell* **142**, 661-667, doi:10.1016/j.cell.2010.08.023 (2010).
- 24 Pincus, D., Letunic, I., Bork, P. & Lim, W. A. Evolution of the phospho-tyrosine signaling machinery in premetazoan lineages. *Proc Natl Acad Sci U S A* **105**, 9680-9684, doi:10.1073/pnas.0803161105 (2008).
- 25 Manning, G., Plowman, G. D., Hunter, T. & Sudarsanam, S. Evolution of protein kinase signaling from yeast to man. *Trends in biochemical sciences* **27**, 514-520 (2002).
- 26 Taylor, S. S., Radzio-Andzelm, E. & Hunter, T. How do protein kinases discriminate between serine/threonine and tyrosine? Structural insights from the insulin receptor protein-tyrosine kinase. *FASEB journal : official publication of the Federation of American Societies for Experimental Biology* **9**, 1255-1266 (1995).
- 27 Hantschel, O. & Superti-Furga, G. Regulation of the c-Abl and Bcr-Abl tyrosine kinases. *Nature reviews. Molecular cell biology* **5**, 33-44, doi:10.1038/nrm1280 (2004).

- 28 Berg, L. J., Finkelstein, L. D., Lucas, J. A. & Schwartzberg, P. L. Tec family kinases in T lymphocyte development and function. *Annual review of immunology* **23**, 549-600, doi:10.1146/annurev.immunol.22.012703.104743 (2005).
- 29 Brauer, P. M. & Tyner, A. L. RAKing in AKT: a tumor suppressor function for the intracellular tyrosine kinase FRK. *Cell cycle* **8**, 2728-2732 (2009).
- 30 Roskoski, R., Jr. Src protein-tyrosine kinase structure and regulation. *Biochem Biophys Res Commun* **324**, 1155-1164, doi:10.1016/j.bbrc.2004.09.171 (2004).
- 31 Huse, M. & Kuriyan, J. The conformational plasticity of protein kinases. *Cell* **109**, 275-282 (2002).
- 32 Sun, G. & Budde, R. J. Expression, purification, and initial characterization of human Yes protein tyrosine kinase from a bacterial expression system. *Archives of biochemistry and biophysics* **345**, 135-142, doi:10.1006/abbi.1997.0236 (1997).
- 33 Lee, S., Lin, X., Nam, N. H., Parang, K. & Sun, G. Determination of the substrate-docking site of protein tyrosine kinase C-terminal Src kinase. *Proc Natl Acad Sci U S A* **100**, 14707-14712, doi:10.1073/pnas.2534493100 (2003).
- 34 Cance, W. G. *et al.* Rak, a novel nuclear tyrosine kinase expressed in epithelial cells. *Cell growth & differentiation : the molecular biology journal of the American Association for Cancer Research* **5**, 1347-1355 (1994).
- 35 Armistead, P. M. & Thorp, H. H. Electrochemical detection of gene expression in tumor samples: overexpression of Rak nuclear tyrosine kinase. *Bioconjugate chemistry* **13**, 172-176 (2002).
- 36 Sheng, Z. M. *et al.* Multiple regions of chromosome 6q affected by loss of heterozygosity in primary human breast carcinomas. *British journal of cancer* **73**, 144-147 (1996).

- 37 Yim, E. K. *et al.* Rak functions as a tumor suppressor by regulating PTEN protein stability and function. *Cancer cell* **15**, 304-314, doi:10.1016/j.ccr.2009.02.012 (2009).
- 38 Zhang, P. *et al.* Regulated association of protein kinase B/Akt with breast tumor kinase. *J Biol Chem* **280**, 1982-1991, doi:10.1074/jbc.M412038200 (2005).
- 39 Barker, K. T., Jackson, L. E. & Crompton, M. R. BRK tyrosine kinase expression in a high proportion of human breast carcinomas. *Oncogene* **15**, 799-805, doi:10.1038/sj.onc.1201241 (1997).
- 40 Robinson, D. R., Wu, Y. M. & Lin, S. F. The protein tyrosine kinase family of the human genome. *Oncogene* **19**, 5548-5557, doi:10.1038/sj.onc.1203957 (2000).
- 41 Wang, J. Y. Controlling Abl: auto-inhibition and co-inhibition? *Nature cell biology* **6**, 3-7, doi:10.1038/ncb0104-3 (2004).
- 42 Nagar, B. *et al.* Structural basis for the autoinhibition of c-Abl tyrosine kinase. *Cell* **112**, 859-871 (2003).
- 43 Demain, A. L. & Vaishnav, P. Production of recombinant proteins by microbes and higher organisms. *Biotechnology advances* **27**, 297-306, doi:10.1016/j.biotechadv.2009.01.008 (2009).
- 44 Studier, F. W. Protein production by auto-induction in high density shaking cultures. *Protein expression and purification* **41**, 207-234 (2005).
- 45 Seeliger, M. A. *et al.* High yield bacterial expression of active c-Abl and c-Src tyrosine kinases. *Protein Sci* **14**, 3135-3139, doi:10.1110/ps.051750905 (2005).
- 46 Jana, S. & Deb, J. K. Strategies for efficient production of heterologous proteins in *Escherichia coli*. *Applied microbiology and biotechnology* **67**, 289-298, doi:10.1007/s00253-004-1814-0 (2005).

- 47 Wang, W. *et al.* Structural characterization of autoinhibited c-Met kinase produced by coexpression in bacteria with phosphatase. *Proc Natl Acad Sci U S A* **103**, 3563-3568, doi:10.1073/pnas.0600048103 (2006).
- 48 Joseph, R. E. & Andreotti, A. H. Bacterial expression and purification of interleukin-2 tyrosine kinase: single step separation of the chaperonin impurity. *Protein expression and purification* **60**, 194-197, doi:10.1016/j.pep.2008.04.001 (2008).
- 49 Esposito, D. & Chatterjee, D. K. Enhancement of soluble protein expression through the use of fusion tags. *Current opinion in biotechnology* **17**, 353-358, doi:10.1016/j.copbio.2006.06.003 (2006).
- 50 Terpe, K. Overview of bacterial expression systems for heterologous protein production: from molecular and biochemical fundamentals to commercial systems. *Applied microbiology and biotechnology* **72**, 211-222, doi:10.1007/s00253-006-0465-8 (2006).
- 51 Amrein, K. E. *et al.* Purification and characterization of recombinant human p50csk protein-tyrosine kinase from an Escherichia coli expression system overproducing the bacterial chaperones GroES and GroEL. *Proc Natl Acad Sci U S A* **92**, 1048-1052 (1995).
- 52 Haacke, A., Fendrich, G., Ramage, P. & Geiser, M. Chaperone over-expression in Escherichia coli: apparent increased yields of soluble recombinant protein kinases are due mainly to soluble aggregates. *Protein expression and purification* **64**, 185-193, doi:10.1016/j.pep.2008.10.022 (2009).
- 53 Tang, Y. C. *et al.* Structural features of the GroEL-GroES nano-cage required for rapid folding of encapsulated protein. *Cell* **125**, 903-914, doi:10.1016/j.cell.2006.04.027 (2006).

- 54 Structural Genomics, C. *et al.* Protein production and purification. *Nature methods* **5**, 135-146, doi:10.1038/nmeth.f.202 (2008).
- 55 Fabian, M. A. *et al.* A small molecule-kinase interaction map for clinical kinase inhibitors. *Nature biotechnology* **23**, 329-336, doi:10.1038/nbt1068 (2005).
- 56 Carter, T. A. *et al.* Inhibition of drug-resistant mutants of ABL, KIT, and EGF receptor kinases. *Proc Natl Acad Sci U S A* **102**, 11011-11016, doi:10.1073/pnas.0504952102 (2005).
- 57 Shah, N. P. *et al.* Overriding imatinib resistance with a novel ABL kinase inhibitor. *Science* **305**, 399-401, doi:10.1126/science.1099480 (2004).

MANUSCRIPT 1

Prepared for submission to Protein Expression and Purification

Bacterial expression, purification and characterization of activated kinase, SRMS: a novel protocol to avoid chaperone protein co-purification

Alex Brown¹ and Gongqin Sun^{1*}

(1) Department of Cell & Molecular Biology, University of Rhode Island – Center for Biotechnology and Life Science, 120 Flagg Road, Kingston, RI 02881.

* Correspondence should be addressed to: gsun@uri.edu, +1-401-874-5937.

Abstract:

Although recombinant expression in bacterial cells offers a convenient and rapid way for producing proteins and enzymes for biochemical and structural characterization, the expression and purification of each kinase often presents its own challenges. Protein-tyrosine kinase SRMS belongs to the Brk family of kinases. The other members of this kinase family, FRK and Brk, have been shown to regulate cell proliferation and survival, and are associated with cancer development. Yet, biochemically, this family has not been extensively characterized. Here we report a procedure for the bacterial expression and purification of SRMS. To overcome the toxicity of SRMS expression, the kinase is co-expressed with the catalytic domain of protein-tyrosine phosphatase 1B (PTP1B). To help overexpressed SRMS fold into the active enzyme, GroES and GroEL chaperones were also co-expressed. However, GroEL binds tightly to SRMS, resulting in extensive GroEL contamination in purified SRMS. The tight binding between SRMS and GroEL is disrupted by a novel washing procedure that includes KCl, ATP-Mg complex, and casein. The purified enzyme is activated by extensive autophosphorylation in the activation loop, and treatment with a protein tyrosine phosphatase, or mutation of the activation loop Tyr, results in the inactivation of SRMS. Several purified enzyme constructs and mutant forms of this kinase were kinetically characterized, yielding regulatory insight.

Keywords: protein-tyrosine kinase SRMS; GroEL; chaperone; casein; dasatinib; autophosphorylation

Introduction:

SRMS, short for Src-related kinase lacking C-terminal regulatory tyrosine and N-terminal myristoylation sites, was originally identified in mice and rats as a novel protein-tyrosine kinase (PTK).[1, 2] Alternatively known as Srm or PTK70, the gene encoding this kinase is also present in humans, located on human chromosome 20q13.3.[3, 4] A double deletion of the mouse SRMS gene showed no readily apparent defects.[1] However, this gene is located on a segment of the chromosome that is known to be frequently amplified in breast cancers and other pathologies.[5-8] Analysis of SRMS mRNA transcripts indicates a ubiquitous expression profile that is especially strong in the skin, as well as regions of the brain, liver, lungs, testes, and gastrointestinal tract.[1, 2]

SRMS and its closest homologs, Brk and Frk, are the only members of the Brk family in humans and other mammals. This group was formerly considered part of the Src Family Kinases (SFKs), on account of their protein sequence homology and common domain architecture. However, conserved exon/intron organization supports their distinction from SFKs as a related, but unique, family of kinases.[6] The functional and biochemical nature of SFKs has been extensively characterized for their importance in cancer biology. Like the SFKs, the oncogenic potential of Brk and Frk has been clearly established.[6, 9] However, this role has yet to be reconciled with evidence suggesting that each of these two BFK members can operate as a tumor suppressor in certain contexts.[10, 11] Through ongoing functional and biochemical studies of Brk and Frk, our understanding of this unique kinase family

continues to evolve. Yet, how SRMS, the remaining BFK member, relates to Brk and Frk is unknown. Since its discovery, no published studies have focused on SRMS, despite its broad expression profile and implicit association with oncogenesis.

SFKs are regulated by two main mechanisms: autophosphorylation of the activation loop on Y416 and C-terminal tail phosphorylation on Y527 (using chicken Src numbering). SFKs become activated by Y416 autophosphorylation and inhibited by Y527 phosphorylation. These opposing regulatory features work in concert to achieve proper kinase activity.[12] SRMS and the rest of the Brk family possess an activation loop Tyr (Y395 of SRMS) but the surrounding sequence varies significantly amongst each BFK member and bears little resemblance to SFKs. Moreover, BFKs lack significant features that are required for tail Tyr phosphorylation in SFKs and SRMS does not possess a C-terminal tail Tyr at all. Given these apparent differences with SFKs, it is unclear how either of these known regulatory mechanisms contributes to activity in BFKs, especially SRMS.

We sought to express and purify SRMS for biochemical characterization. Recombinant expression in *E. coli* is often convenient for the *in vitro* analysis of PTKs because it is rapid and relatively inexpensive; but it is not without its challenges. In the expression and purification of SRMS, we circumvented problems of toxicity and solubility by co-expressing a protein-tyrosine phosphatase and GroES/GroEL chaperone proteins, respectively. Tight binding between SRMS and GroEL was dissolved by new washing procedures with ATP-Mg complex and casein. To validate this system, we generated various wild-type and mutant kinase constructs for *in vitro*

assays. The biochemical data obtained from this initial characterization of SRMS demonstrates that this kinase is activated by autophosphorylation, providing insight into the regulation of this poorly understood protein-tyrosine kinase family. Thus, this system offers a convenient and reliable means to derive active SRMS that is suitable for biochemical studies of regulation and is likely adaptable to many other protein-tyrosine kinases. Furthermore, the unique washing procedure presented provides a useful tool for the removal of co-purifying GroEL, a common obstacle to the purification of a wide variety of proteins.

Table 1.Components of the bacterial expression system for SRMS purification.^a

Plasmid	Product	Resistance	Function
<i>pGEX4T1-SRMS</i> ^b	GST-SRMS fusion protein	ampicillin	Target kinase with an affinity-tag
<i>pCDF-MBP-PTP1B</i>	MBP-PTP1B fusion protein	streptomycin	PTP 1B to reduce toxicity of heterologous PTKs
<i>pREP4-GroESL</i>	GroES and GroEL	kanamycin	Chaperones to increase solubility of target kinase
<i>pRIL</i>	<i>argU</i> , <i>ileY</i> , and <i>leuW</i> tRNAs	chloramphenicol	Rare tRNAs to enhance SRMS translation

^a *Escherichia coli* BL21(DE3) was used as the host strain.^b Full-length (FL), catalytic domain (Cata), and unique domain-deletion (D60) forms of SRMS were used.

Materials and Methods:

Reagents and chemicals

Consumables and culture media, or media components, were purchased from Fisher Scientific. Dasatinib was purchased as free base from LC laboratories, the PY20 anti-phosphotyrosine antibody was purchased from Santa Cruz, and ³²P-labeled ATP was from Perkin-Elmer. All other chemical reagents were purchased from Sigma-Aldrich.

Molecular cloning and recombinant expression of SRMS

The full-length, Δ60 (removing unique domain), and the catalytic domain forms of rat SRMS (NCBI: NM_001011961) were cloned from commercially available, plasmid-encoded cDNA using custom primers. Digestion and ligation with the pGEX-4T-1 plasmid was followed by transformation to our host strain. DNA sequencing results confirmed that SRMS was properly inserted along the reading frame of the N-terminal GST affinity tag (Figure 1). Custom primers were used in site-directed mutagenesis of WT to Y395F (activation loop Tyr to Phe) using standard QuikChange (Agilent) protocols and confirmed via sequencing. The host strain of *E. coli* BL21(DE3)-RIL was previously transfected with separate plasmids encoding PTP1B phosphatase and GroES/GroEL chaperone proteins to reduce kinase toxicity and promote solubility of the recombinant kinase (Table 1). Previously, this host has proven successful for the rapid production of highly purified recombinant PTKs.[13, 14]

Figure 1.

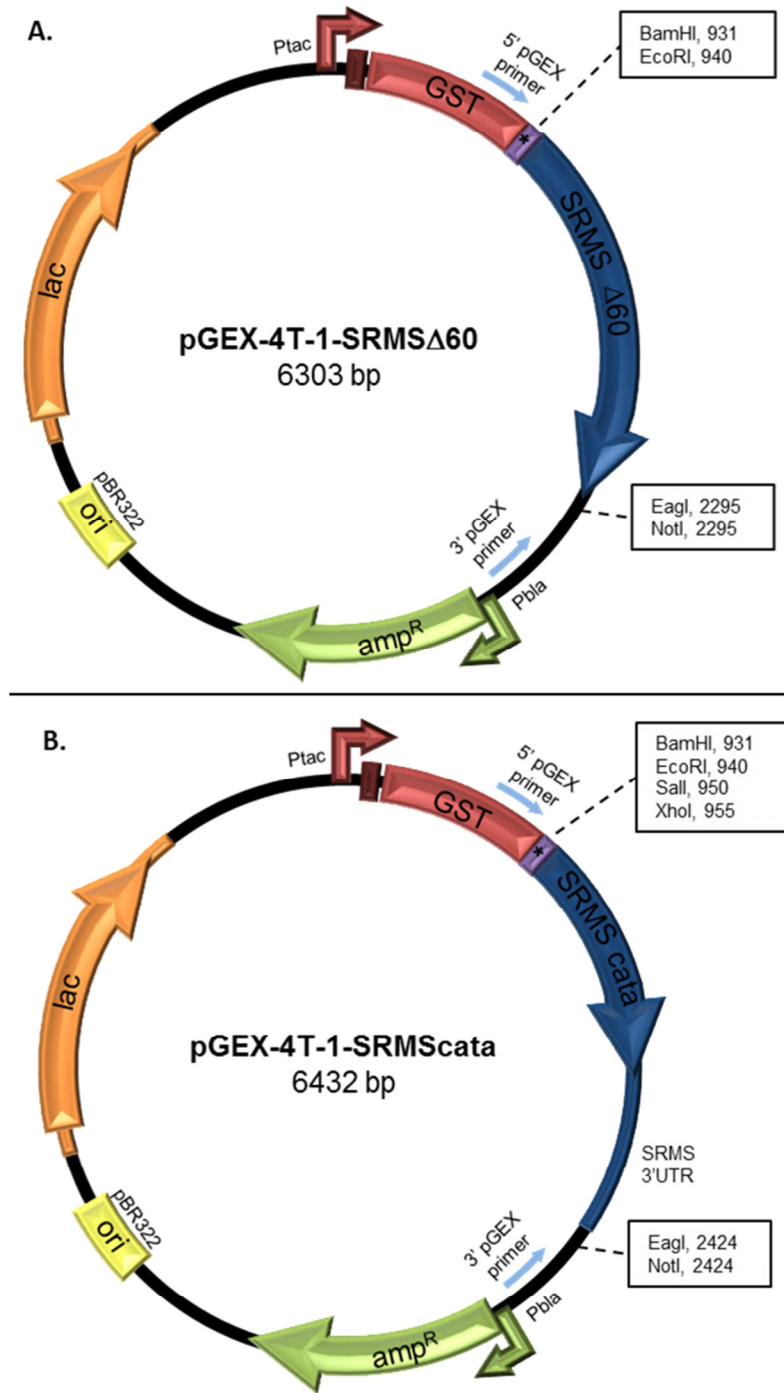


Figure 1 – Expression vector design and cloning. SRMS cDNA was PCR amplified from rat cDNA using custom primers to incorporate the sites necessary for restriction digestion and cloning. SRMS was successfully cloned for inducible expression and purification as GST-fusion proteins from the following constructs: pGEX-4T-1-SRMS Δ 60, **A**, does not contain the N-terminal Unique domain (first 60 residues) but contains all other coding regions including the SH3, SH2, and catalytic domains; pGEX-4T-1-SRMS_{cata}, **B**, contains the catalytic domain of SRMS and the gene's native 3' un-translated region (3'UTR). pGEX-4T-1-SRMS-FL was also cloned but did not yield significant quantities of the full-length enzyme. The unique restriction enzyme cut sites outside of the coding regions are shown (boxed), indicating their cut sites within the vector.

Bacterial culturing was performed while shaking at 250 rpm in 37°C LB media containing the appropriate antibiotics. Freshly plated colonies were used to grow overnight cultures and, in the morning, these were diluted at least 50-fold into 500mL of pre-warmed media in two 1-liter flasks. For optimal culture and induction, we employed the auto-induction method, described by Studier. [15] In this method, cultures are grown shaking at 37°C until an OD₆₀₀ of 1.0-2.0 was reached, transferred to room temperature, and then grown for about 24 hours, until the growth plateaued (typically OD₆₀₀ = ~14). Cells were harvested at 4°C by centrifuging the culture at 9,000 x g for 6 minutes. Cell pellets were then frozen at -20°C overnight or stored less than a week prior to purification of the expressed SRMS.

Optimized protein purification procedure

Cell pellets were thawed and resuspended on ice in 1/10 original culture volume of pre-chilled PBS lysis buffer, consisting of 80 mM phosphate, 600 mM NaCl, 0.1% β-mercaptoethanol, 1 mM EDTA, and 0.01% triton X-100 at pH of 7.3. These high phosphate and salt concentrations were found to drastically improve GST-SRMS solubility. Following resuspension, lysozyme was added to a concentration of 0.1 mg/mL and incubated on ice for 10-20 minutes, prior to sonication. While on ice, lysates were sonicated in four 30-second increments between setting 3 and 4. Lysates were cleared by centrifugation at 22,000 x g for 10 min in 4°C. After reserving a small sample for later analysis, the supernatant was then incubated with ~1mL of pre-swollen GSH-agarose bead (Sigma) while shaking at 4°C. After one hour, the

lysate suspension was passed through an empty chromatography column and a sample of the flow-through was collected and preserved for later analysis. Washing of the column was carried out at 4°C using 50 mL of wash buffer A (80mM phosphate, 600mM NaCl, 0.1% β-mercaptoethanol, pH of 7.3) and then followed by 40 mL of wash buffer B (50 mM Tris, 0.1% β-mercaptoethanol, pH of 7.3).

To remove GroEL, supplementary wash buffers were used. The AMK wash buffer was freshly prepared to contain 5mM disodium ATP, 10mM MgCl₂, 150mM KCl, 0.1% β-mercaptoethanol, and 50mM Tris at a pH of 7.3. For most effective GroEL washing, our optimized procedure utilizes AMK washing buffer + casein. 50mg/mL lyophilized casein was prepared as a stock solution of 1M NaOH by intermittently vortexing at room temperature and then diluted 100-fold in the AMK washing buffer and pH adjusted to 7.3 with HCl for a final concentration of 0.5mg/mL. GroEL was removed from the column by re-suspending the resin with AMK + casein, incubating for 5-10 minutes (just long enough for the bead to re-settle), and then allowing the wash to pass through the column. This step was repeated every 10-15mL's of washing solution to effectively release GroEL with just 50mL of AMK/Casein buffer. The SRMS-bound agarose was then rinsed with a final volume of 50mM Tris (pH 8) + 0.1% β-mercaptoethanol to remove lingering washing buffer components, and GST-SRMS was eluted in the same buffer, plus 10mM reduced glutathione. Protein concentration was quantified via Bradford assay according to a standard BSA curve prior to storage at -20°C as diluted 40% glycerol working stocks.

SDS-PAGE and Western Blotting

Protein purity was assessed by SDS-PAGE and Coomassie staining. Samples were mixed with one-third volume Laemmli sample buffer containing 2.5% β -mercaptoethanol, heated for 10 min at 95°C, and centrifuged at >13,000 rpm on a table-top centrifuge for 30 seconds prior to loading. Except where noted, SDS-PAGE was carried out using Bio-Rad Criterion XT 4-12% polyacrylamide Bis-Tris pre-cast gels with MOPS running buffer accompanied by pre-stained Precision-Plus Kaleidoscope molecular weight standards. Gels were resolved for 45-60 minutes at a constant 200V before Coomassie staining for 30 minutes. Following de-staining and equilibration in water, gels were imaged and analyzed with the Bio-Rad GelDoc system.

For western analysis, samples were first subjected to SDS-PAGE, as described above. Gels were equilibrated in transfer buffer and then blotted onto methanol-activated polyvinylidene difluoride (PVDF) membranes for one hour at 25V using a semi-dry transfer apparatus. Proper quantitation of the samples was confirmed by Coomassie staining a duplicate gel or Ponceau S treatment of the membrane. Thorough and even transfer of the samples to the PVDF membrane was visually verified from the spent protein gel. Membranes were immediately blocked in TBST containing 5% non-fat milk for one hour at room temperature and then rinsed with TBST. The membranes were immunoblotted with mouse monoclonal anti-phosphotyrosine IgG (PY20, Santa Cruz) and HRP-conjugated mouse IgG antiserum, with washing in TBST in between the primary and secondary antibody treatments.

Blots were examined after 5 minutes treatment with ECL+ substrate (GE Healthcare) by exposure to film.

Kinase Assays

All kinase assays were carried according to previously published protocols. Duplicate 40 μ L samples, each containing the appropriate enzyme/sample concentration and 1mg/mL polyE₄Y substrate, were prepared in kinase buffer (75mM EPPS, pH 8.0 + 5% glycerol + 0.005% Triton X-100) prior to the assay. Reactions were initiated by addition of 10 μ L ATP-Mg cocktail for a final concentration of 200 μ M ATP/[γ -³²P]-ATP and 12 mM MgCl₂. The specific activity (usually between 750 and 1,500 dpm/pmol) of each assay's reactions was kept constant. All reactions were incubated at 30°C for 20 min, then 35 μ L of each reaction was spotted onto 1- x 2-cm strips of filter paper, which were then washed in 5% trichloroacetic acid (65°C, constant stirring). The ³²P incorporation into PolyE₄Y was quantified using a Beckman Coulter LS-6500.[16]

For kinase assays designed to determine the K_m, the reactions were setup as described above except the concentration of ATP in each reaction was varied (but not the specific activity). To determine inhibitor IC₅₀'s, dasatinib was dissolved in 10% DMSO, diluted in series, and included within the kinase reactions. For kinetic analysis of turnover, K_m, and IC₅₀ determination, each kinase assay was performed in duplicate and repeated at least three times. All calculations and data treatment of

assay results, including double reciprocal plots and linear regression analysis, was carried out in Microsoft Excel.

Results and Discussion:

Recombinant expression system for SRMS

Currently, the only published reports of SRMS enzymatic activity utilize commercially produced wild-type catalytic domain from insect cell expression systems. As we aim to characterize SRMS regulation, we opted to develop a bacterial expression system that would enable efficient mutational analysis. To this end, we cloned the coding sequence of SRMS into the multiple cloning site of pGEX-4T-1 to express the kinase as a fusion protein of GST-SRMS (Figure 1). However, there are several challenges to expressing and purifying protein-tyrosine kinases from a bacterial system.

Some PTKs are toxic to bacterial hosts because they tend to phosphorylate many native proteins. Co-expression of a protein tyrosine phosphatase, such as PTP1B, often helps to overcome this problem.[17, 18] Additionally, expression in bacteria may cause recombinant enzymes to fold incorrectly, leading to insolubility and limiting activity. This problem is frequently alleviated by the co-expression of chaperone proteins, such as GroES/GroEL. Finally, the frequency of codon usage varies substantially from human to bacteria and this is thought to have negative influence on the total yield of target proteins. A PTK with many codons that are rarely used in bacteria may not be well expressed due to insufficient host production of certain aminoacyl-tRNA.

To mitigate this problem, host strains are often complemented with plasmids, such as pRIL, which elevate rare tRNA for Arg, Ile, and Leu, to greatly enhance

expression.[19] With these considerations in mind, we co-expressed SRMS with PTP1B, GroES/EL, and Arg/Ile/Leu tRNAs to increase the quantity and quality of the recombinant enzyme produced by the *E. coli* BL21(DE3) host strain. The components of this system are detailed in Table 1, and similar expression strategies have been used in the past for SFKs, as well as other kinases.[13, 14]

Purification of active SRMS

Our initial attempts using this system relied on traditional IPTG induction and GST affinity purification. This, however, resulted in low yields and the co-purification of significant amounts of the chaperone GroEL alongside the kinase in the eluted fractions. We then switched to an auto-induction protocol, proven to increase the yield of many recombinant proteins.[15] Using this method greatly enhanced the apparent solubility and yield of SRMS; however, the chaperone impurity remained problematic, despite extensive washing (over 200 mL of wash buffers A and B).

Co-purification of chaperones is a common phenomenon and often occurs despite optimization of induction and purification conditions. In these instances, dissociation of the complex is most often readily achieved by introducing ATP-Mg²⁺ and/or denatured protein to various steps in the purification. The ATP-Mg²⁺ is thought to induce conformational changes of the chaperone, promoting the release of bound protein. However, published literature lacks a procedure that is suitable for all PTKs.

In the purification of ITK, a Tec family kinase, the Andreotti lab, encountered a similar problem. They found that adding potassium (150 mM KCl) to a solution of ATP-Mg²⁺ (AMK washing buffer) effectively released enough of the bound GroEL to attain sufficient ITK purity.[18] We adapted and optimized this protocol for the purification of SRMS.

As seen in Figure 2, GroEL (~60 kD) appears to be the dominate protein within the soluble cell lysate, shown in lane 1. A significant portion of GroEL appears to be removed during the initial stages of purification, as evidenced by lane 2, which contains the unbound lysate column flow-through. Following extensive application of wash buffers A and B (200 mL total), until no protein can be detected from the column flow-through, the column was stoppered, moved to room temperature, and 5 mL of AMK solution was used to re-suspend the resin. After 5-10 min incubation, the stopper was removed and the first 0.5 mL of the wash buffer flow-through was collected for analysis, followed washing with an additional 25 mL AMK buffer. This incubation and wash step was repeated six more times. Examining these wash fractions (lanes 3 – 9), it is clear that the AMK solution removes a significant amount of GroEL that wash buffers A and B were unable to remove. After approximately 200 mL of AMK wash (lane 9), very little GroEL is cleared from the column. However, upon elution of GST-SRMS with 10mM reduced glutathione, lanes 10 – 12, it is clear that the AMK wash was only partially effective at removing GroEL and its efficacy appears to increase with respect to the volume of buffer applied to the column.

Figure 2.

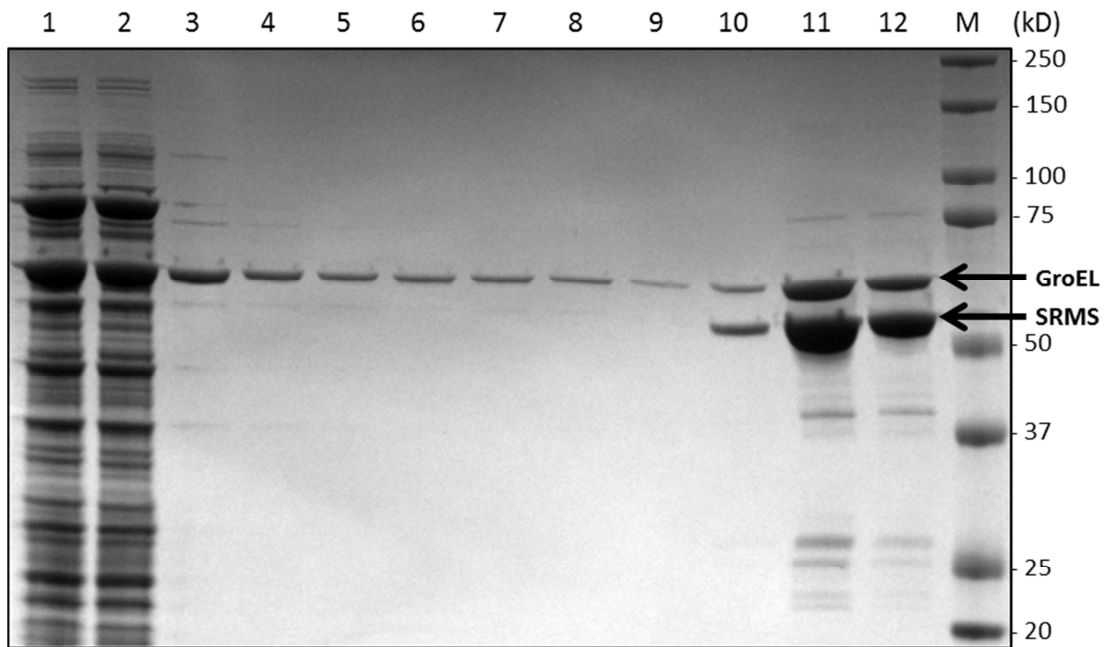


Figure 2. Purification of GST-SRMS using existing purification procedure. As described in the Materials and Methods section, a previously published procedure was adapted for our initial attempts to purify SRMS. Proteins from various steps of the purification were sampled (20 μ L) for separation by SDS-PAGE and stained with Coomassie Blue for analysis. Lane 1, soluble cell lysate; lane 2, flow-through from initial loading; lanes 3 – 9, consecutive washing steps (30 mL each) with AMK buffer; lanes 10 – 12, fractions eluted with 10mM GSH elution buffer; lane M, molecular weight markers labeled by size (kD).

These results lead us to seek out additional wash buffer additives to more effectively remove the chaperone protein. Several studies have suggested that casein, a common milk protein, can interact with GroEL through hydrophobic interactions to promote specific molecular rearrangement and facilitate the binding/release of ATP/ADP. Yet, to date, no purification protocol has made use of casein as an effective washing reagent.[20-22] In light of these reports, we experimented with casein at various points within the standard GST-tag purification procedure, including it in the lysis buffer and as a supplement to normal washing buffer. Following extensive washing with buffers A and B, wash buffer B + casein was applied to the column. A sample of this wash fraction was run in lane 4 of Figure 3A. In this lane, little to no GroEL appears to have been cleared from the resin, which indicates that either casein in the wash buffer is unable to displace GroEL, or that casein in the lysis buffer had prevented the chaperone from ever binding GST-SRMS. To investigate further, the residual casein was removed by washing with buffer B (lane 5) and then washed with AMK buffer. Since the AMK wash was shown to be partially effective at clearing GroEL from the column (see Figure 2), the absence of the contaminant from this fraction would indicate that casein is at least partially effective at preventing GroEL from binding the column. However, GroEL is clearly released by this AMK wash (lane 6) indicating that a significant amount of the chaperone remains on the column. From these results, it can be concluded that casein, on its own, is ineffective at preventing or disrupting the interactions of GroEL with both free and column-bound GST-SRMS.

Figure 3.

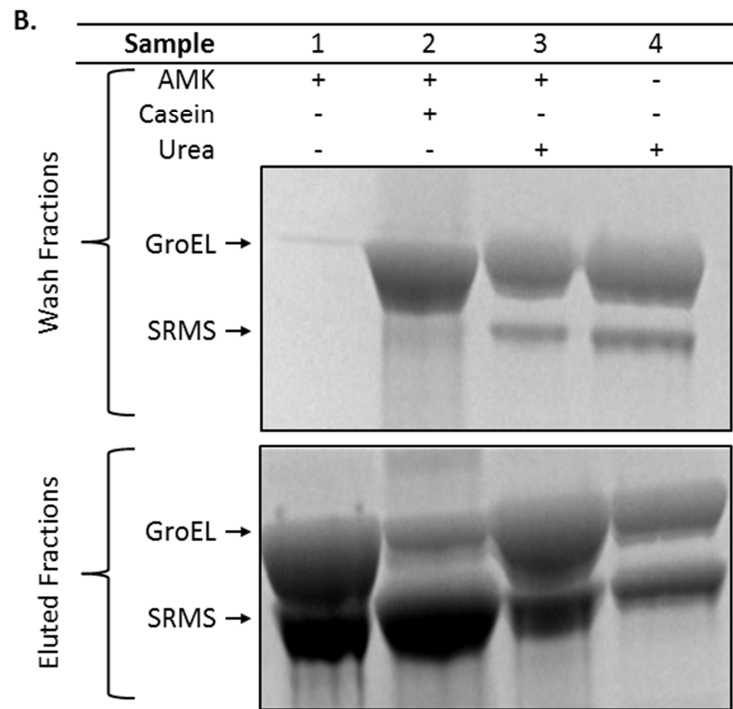
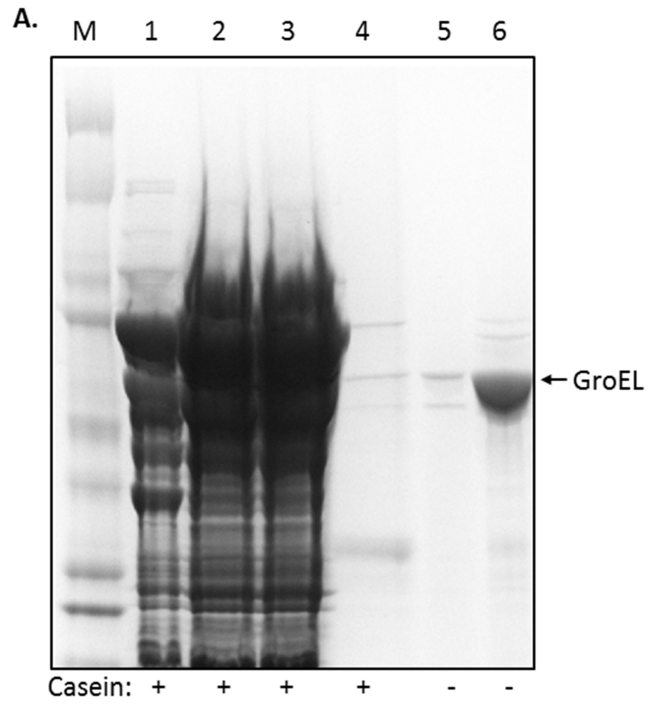


Figure 3. Optimization of washing to remove GroEL. **A.** Casein was added to the standard lysis and wash buffers (0.5 mg/mL each) and the GST-SRMS purification procedure was followed as described in Materials and Methods, stopping short of elution. 20 μ L samples of each step were taken for analysis by SDS-PAGE and Coomassie Blue staining. Lane M, molecular weight markers; lane 1, insoluble cell pellet; lane 2, soluble cell lysate; lane 3, flow-through from initial loading; lane 4, washing buffer + casein; lane 5, washing buffer; lane 6, AMK washing buffer. **B.** Following thorough AMK washing, GSH-agarose bound by GST-SRMS was divided into four different spin columns for wash buffer component optimization, prior to elution with 10mM GSH elution buffer. The wash and eluted fractions of each sample were then examined via SDS-PAGE and Coomassie Blue staining. Sample 1, washed with AMK buffer; sample 2, washed with AMK buffer + 0.5 mg/mL casein; sample 3, washed with AMK buffer + 2M urea; sample 4, washed with 2M urea.

Hypothesizing that ATP may be required for casein to effectively interact with GroEL, we investigated casein's prospective use in the context of the AMK washing buffer procedure. GSH-Agarose resin, bound by GST-SRMS, was washed extensively with AMK buffer. 100 μ L of this pre-washed resin was loaded into spin columns and further subjected to washes of the following conditions: 1) AMK, 2) AMK + 0.5 mg/mL casein, 3) 2M urea, or 4) 2M urea + AMK. Figure 3B reveals both, proteins that are washed off (top) and proteins that remain bound to the column (bottom), following these supplementary washes. The sample that was washed with additional AMK buffer shows no further GroEL is released by this method (top panel, lane 1). Thus, as expected, the corresponding eluted sample contained a significant amount of GroEL impurity (bottom panel, lane 1). At the concentration used, urea has been shown to mildly destabilize the structure of GroEL and was thus used in an attempt to differentially elute it from the column. Unfortunately, the urea washes appeared to elute significant amounts of GST-SRMS alongside GroEL (top panel, lanes 3 and 4). The AMK + casein wash, however, released a substantial amount of GroEL with little to no SRMS loss (top panel, lane 2). As indicated by the eluted fractions (bottom panel, lane 2), the combination of casein with AMK buffer appears to preferentially remove GroEL to drastically improve the ratio of SRMS to GroEL.

Based on these results, we have devised an optimized procedure that is described in detail within the methods section of this report. In summary, plasmids encoding GST-SRMS, GroEL/GroES, and PTP1B were transformed into *E. coli* BL21(DE3)-RIL, grown at 37°C in liquid culture, and then induced at room

temperature via auto-induction. Standard GST affinity purification is then used along with a modified washing protocol that uses a novel AMK + casein buffer for removal of bound GroEL. GST-SRMS can then be eluted from the column, free of any significant impurities. Pooled fractions often contain 2 – 5 mg of active enzyme from half a liter of culture, enough for >1,000 assay reactions, without the need for additional concentration or re-folding steps. SRMS can be stored in 40% glycerol at -20°C for more than a year without significant loss of kinase activity. This strategy was used to purify the catalytic domain and $\Delta 60$ (SH3-SH2-Kinase), as well as their mutants (see Figure 4 and Table 3).

Figure 4.

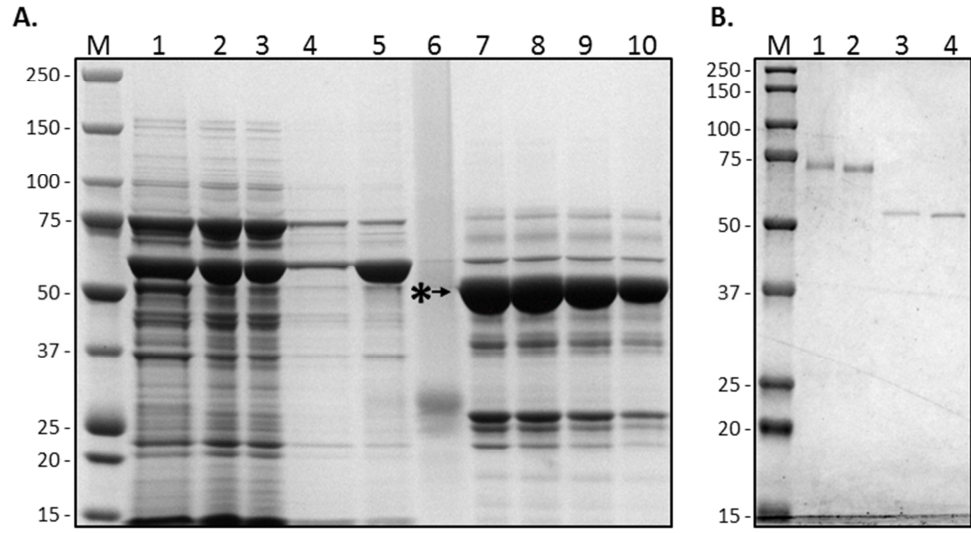


Figure 4. Optimized SRMS purification. GST-SRMS was purified as described in the Materials and Methods and samples from various points of the purification were analyzed by SDS-PAGE and Coomassie staining. **A.** Wild-type catalytic domain of SRMS purification: lane M, molecular weight markers; lane 1, 50µg insoluble cell pellet; lane 2, 50 µg soluble cell lysate; lane 3 50 µg flow-through lysate; lane 4, 20 µL standard wash step; lane 5, 20 µL from AMK wash step; lane 6, 20 µL from final buffer wash step; lanes 7-10, 20 µL of the peak eluted fractions (*=SRMS). The peak eluted fractions from **B.** Equimolar amounts (3.5 pmol) of the eluted fractions of GST-SRMS purifications were run together on SDS-PAGE for comparison following Coomassie Blue staining. Lane M, molecular weight markers; lane 1, WT catalytic domain; lane 2, Y395F catalytic domain; lane 3, WT Δ60; lane 4, Y395F Δ60.

Table 2.

Summary of SRMS purification

Step	Total protein ^a (mg)	Total activity ^b (nmol min ⁻¹)	Specific activity (nmol min ⁻¹ mg ⁻¹)	Yield ^c (%)	Purification ^c (fold)
Lysate	1,027	.01	9.29×10^{-6}	100	1
Elution	5.6	16.74	2.99	1,674,000	321,842

^a SRMS was purified from 500 mL bacterial culture as described in Materials and Methods.

^b The SRMS kinase activity was assayed using PolyE₄Y as the substrate.

^c The cell lysate contains significant amounts of PTP1B, a protein tyrosine phosphatase.

Kinetic characterization of SRMS

To establish our purification protocol as a viable means of producing active enzyme, we characterized the kinase activity of the catalytic domain. Kinetic analysis of SRMS was conducted with the generic substrate polyE₄Y (heterogeneous peptide mixture with a 4:1 ratio of Glu and Tyr) and we determined a k_{cat} of 26 min⁻¹ (Table 3). Enzyme turnover from multiple purifications were in good agreement. As no physiological protein substrates have yet been reported for SRMS, a direct comparison of catalytic potential is perhaps best judged by its K_m of ATP, the universal PTK substrate. As determined from the double-reciprocal plot of activity vs. ATP concentration (Figure 5) the K_m_{ATP} was determined to be 40 μ M. This value is significantly lower than those previously determined for Csk (~150 μ M) and Src (~100 μ M). Taken together, the kinetic data clearly indicates strong catalytic activity of SRMS, thus validating our purification methods.

Figure 5.

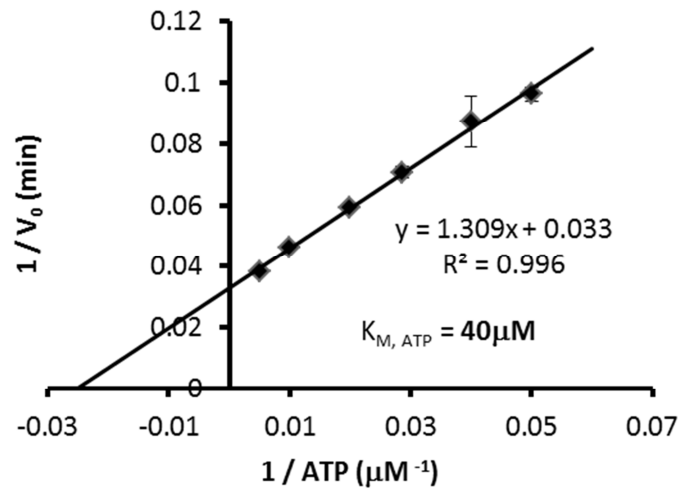
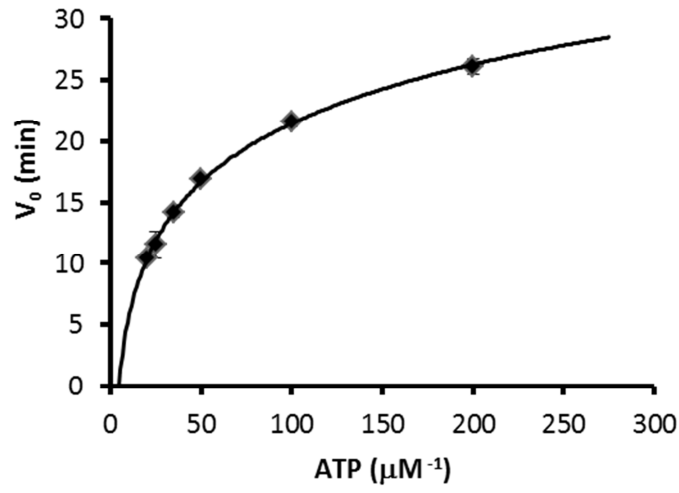


Figure 5. Enzyme kinetics of the purified catalytic domain of SRMS. For K_M of ATP determination, 2.66 nM of SRMS was assayed with concentrations of 20, 25, 35, 50, 100, and 200 mM 32 P labeled ATP using 1 mg/mL PolyE₄Y as substrate.

Table 3.

Enzymatic activity of purified SRMS

SRMS ^a	Turnover ^b (min ⁻¹ ± std.dev.)
Cata WT	26.10 ± 0.62
Cata Y395F	3.12 ± 0.27
D60 WT	1.06 ± 0.10
D60 Y395F	0.26 ± 0.03

^a Purified as GST-fusion proteins.^b Using PolyE₄Y as substrate.^c Y395 corresponds to the activation-loop Tyr.

SRMS autophosphorylation

Most protein-tyrosine kinases are known to autophosphorylate on the Tyr residue of their activation loop, and this phosphorylation tends to activate a kinase. The specific level of this activation, however, is highly variable from one kinase to another and ranges from non-detectable to several hundred-fold. Since little is known of BFK regulation, and because the purification procedure for SRMS required extensive incubation in the presence of ATP-Mg²⁺, it was important to assess how this procedure affected the level of SRMS phosphorylation, and any resulting implications for the overall kinase activity. To fully address this issue, we first expressed and purified an SRMS mutant containing a Phe instead of Tyr at the autophosphorylation site (Y395F). Kinase assays from various purifications indicate that this mutant form of the catalytic domain displays a k_{cat} of 3 min⁻¹, 11.5% of the wild-type activity (Table 3). This result suggests the possibility that this form of WT SRMS is activated by autophosphorylation, during the purification. However, we cannot exclude the possibility that the mutation of the wild-type Tyr to Phe could have directly affected the kinase activity. To further clarify this result, we then tested how incubation with ATP-Mg²⁺ or a protein tyrosine phosphatase affected the Tyr phosphorylation level of SRMS and the Y395F mutant, as well as their corresponding kinase activities.

Shown in Figure 6A, purified WT SRMS catalytic domain (273 µg/mL) was incubated with either kinase buffer (negative control), 200 µM ATP and 12 mM Mg²⁺, or PTP1B for 0, 20, or 60 minutes. The amount of PTP1B was carefully determined so

that, upon dilution for the kinase assay, phosphatase activity was insignificant. To further reduce the chances of PTP1B confounding this experiment, each kinase reaction was performed under non-reducing conditions which are catalytically unfavorable to phosphatases. The protein level in the treated samples was calculated based on pre-determined protein concentrations and molecular weights, and confirmed by SDS-PAGE and Ponceau S staining (bottom panel). The Tyr phosphorylation level in the samples was determined by western blotting with PY20 anti-phosphotyrosine antibody (middle panel). The kinase activities of the treated samples were determined by the kinase activity assay (graphed, top panel). In this series of experiments, the control treatment and incubation with ATP-Mg did not change SRMS Tyr phosphorylation level, nor the kinase activity. However, incubation with PTP1B dramatically decreased Tyr phosphorylation and kinase activity levels. These results together indicate that purified SRMS is fully phosphorylated and activated. These same experiments were performed using the Y395F form of SRMS.

As seen in Figure 6B, the Y395F mutant displays a much lower level of Tyr phosphorylation. Although a low level of phosphorylation suggests at least one additional site of autophosphorylation, treatment with PTP1B failed to decrease the kinase activity level of Y395F SRMS. Overall, by comparison of the anti-phosphotyrosine blots and kinase activities from each treatment of the enzymes, it is apparent that the kinase activity of SRMS strongly correlates to Tyr395 phosphorylation level. The WT SRMS kinase activity was reduced from 16.8 min^{-1} (negative control, 60 min) to approximately 3.2 min^{-1} (60 min, PTP1B treatment). This

represents more than five-fold reduction in activity, despite incomplete dephosphorylation (as indicated by the western blot) and any autophosphorylation that may have occurred during the kinase assay. Altogether, the results seen in Figure 6A and B indicate that activation by autophosphorylation of WT SRMS is achieved, primarily, through phosphorylation of Tyr 395 in the activation loop. Furthermore, these assay results (and several not shown here) suggest that autophosphorylation of the activation loop tyrosine results in approximately 5- to 10-fold activation of SRMS kinase activity.

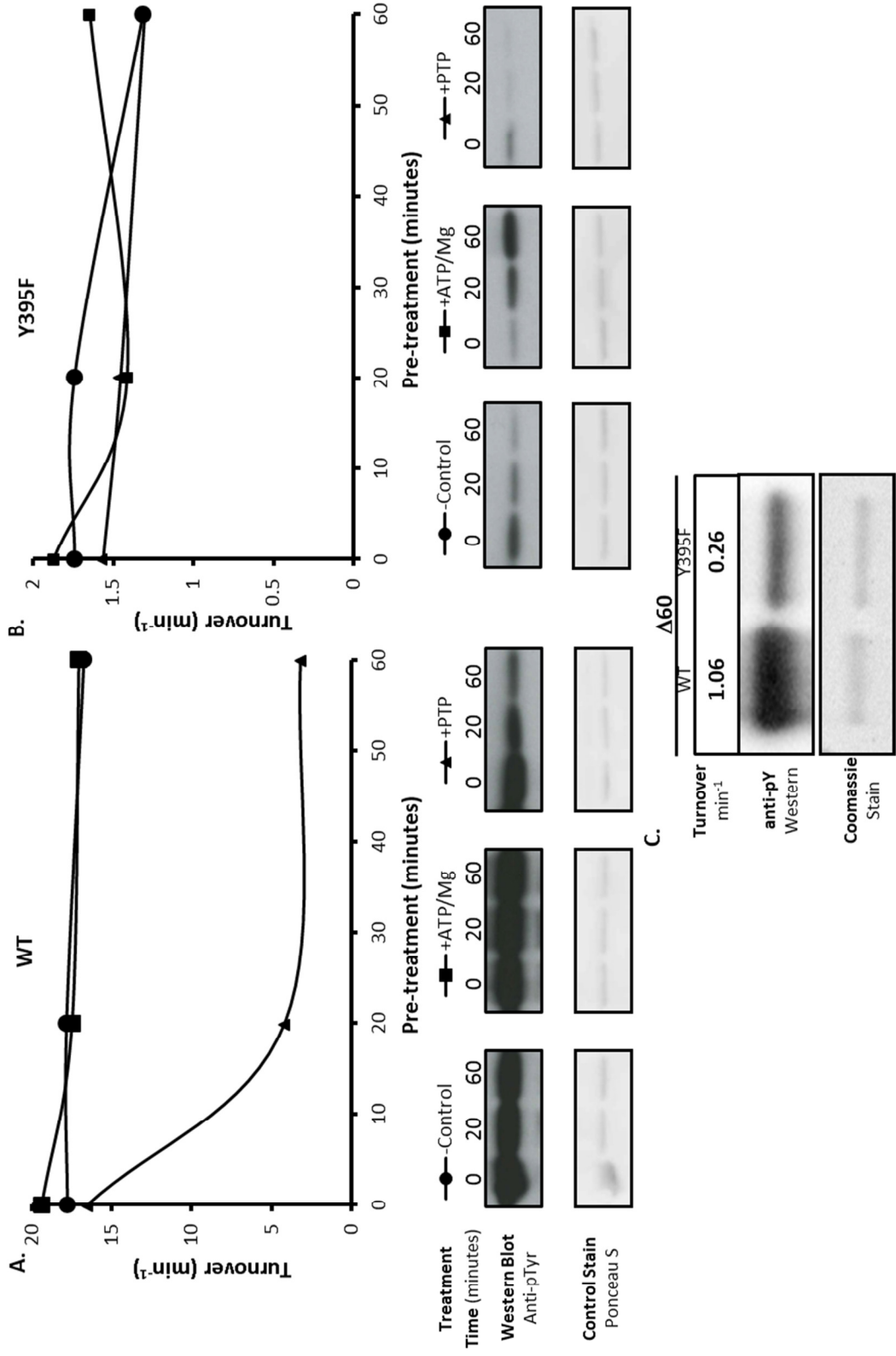


Figure 6.

Figure 6. SRMS autophosphorylation of the activation loop Tyr, Y395. The WT (**A**) and Y395F (**B**) GST-SRMS catalytic domains were pre-treated with either ATP/Mg²⁺, purified PTP1B, or kinase buffer (as a control) for 0, 20, or 60 minutes prior to analysis of phosphorylation and activity. To detect phosphorylation, samples were run on SDS-PAGE before being transferred to PVDF for western blotting with anti-phosphotyrosine antibody (PY20). Membranes were stained with Ponceau S to ensure even sample loading and transfer. The samples were also analyzed for their kinase activity using ³²P-ATP and PolyE₄Y (results in bar graphs) for comparison. Western analysis of untreated WT and Y395F GST-SRMS Δ60 was also carried out, and kinase activity was determined (**C**).

Characterization of $\Delta 60$ WT and Y395F SRMS kinase activity toward polyE4Y yielded turnovers of 1.06 and 0.26 min^{-1} , respectively (Table 3). While substantially less active than the catalytic domain, these values suggest a similar pattern of activation by autophosphorylation. To examine whether the difference in kinase activity between WT and Y395F $\Delta 60$ also correlates to phosphorylation levels, we blotted the WT and mutant forms as described above. Western blot analysis of $\Delta 60$ with anti-phosphotyrosine antibody, shown in Figure 6C, confirms a substantial decrease in phosphorylation of the Y395F SRMS. This is consistent with our results of the catalytic domain and suggests this mode of activation by autophosphorylation is not intrinsically inhibited by the SH3 or SH2 domain.

Additionally, this figure once again demonstrates that SRMS can be phosphorylated on Tyr residues outside of the activation loop. Whether this phosphotyrosine has any impact on the dramatic difference in observed activities of the $\Delta 60$ and the catalytic domain forms of the enzyme is not apparent from our analysis. It is important to note that this study cannot rule out many potential artifacts that could interfere with enzymatic stability, stemming from the inclusion of the SH3-SH2 domains or lack of the unique domain in the $\Delta 60$ SRMS construct. The apparent suppression of $\Delta 60$ activity is none the less intriguing, especially considering that Brk, Frk, the entire Src family, and many other PTKs are negatively regulated by intramolecular SH3 and SH2 domain interactions in phosphotyrosine dependent and independent mechanisms. However, further investigation is clearly needed to

determine whether any of these conserved inhibitory features may be present in SRMS.

Dasatinib inhibition of the active and inactive forms of SRMS

When studying kinases such as SRMS, inhibitors often serve as invaluable research tools. Dasatinib is a broad spectrum PTK inhibitor originally developed to target the Abl catalytic domain, with broad clinical application to cancer therapies. With a sub-nanomolar K_D and IC_{50} , dasatinib has been shown bind to the active form of Abl.[23] This binding mode has been reaffirmed by several other kinase structures, particularly Src, which show comparable affinity to the active conformation. Molecular modeling approaches, however, predict that dasatinib should also be able to bind the active site. Many publications continuously cite dasatinib's ability to bind both inactive and active conformations, despite contrary structural evidence and without any biochemical analysis to support these claims.[24] Because of the inherent difficulties of studying this problem with ABL, these controversial claims persist and have complicated rational drug design efforts. As dasatinib has been shown to bind SRMS with a K_D of 13nM, we sought to examine the inhibitor's capacity to discriminate between the enzyme's active and inactive forms. Also, if this analysis confirms the suspected inhibitory effects of dasatinib upon SRMS, it will also validate dasatinib's potential use in the investigation of this understudied kinase.

The phosphorylation of the activation loop does not always lead to activation of a kinase, as many kinases differ in this regard. All kinases have the ability to adopt

an active conformation, independent of activation loop phosphorylation, with varying efficiency. In particular, ABL appears to convert between these conformations equally well, regardless of autophosphorylation. Because of ABL's inability to become activated in this manner, it is difficult to determine whether dasatinib truly binds either form, or just active conformation kinase. As we have recently demonstrated the capacity of SRMS to achieve activation via autophosphorylation, we subjected both active and inactive forms of the kinase to dasatinib treatments while assaying their kinase activities toward PolyE₄Y. Our analysis results (Figure 7) of the inhibitor toward the catalytic domain of SRMS revealed an IC₅₀ value for the Y395F mutant of 10 nM and the active/phosphorylated WT was found to be 3.5 nM, about a three-fold difference. This clearly demonstrates a preference for the active form, in support of the structural data concerning dasatinib. These values also serve to validate the use of dasatinib as potentially valuable tool or probe, in addition to phosphorylation levels of Y395, for further *in vitro* characterizations and functional analysis of active SRMS.

Figure 7.

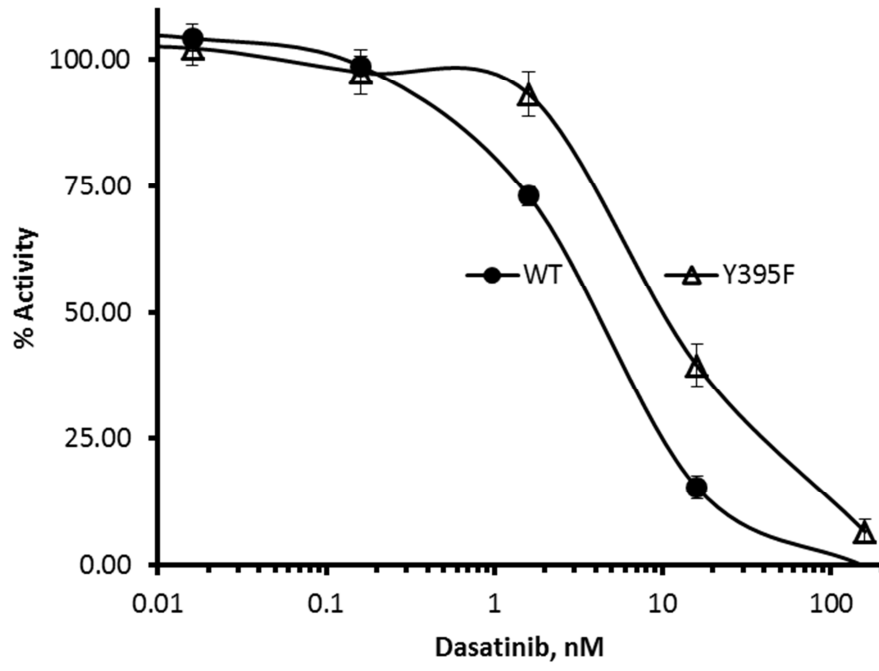


Figure 7. Dasatinib inhibition of the active and inactive forms of SRMS. The activity (turnover, $\text{min}^{-1} \pm$ standard error) of WT and Y395F SRMS catalytic domains were first assayed without inhibitor: WT = 29.15 ± 0.28 ; Y395F = 3.12 ± 0.15 . The activity of each enzyme was then measured in the presence of 160, 16, 1.6, 0.16, and 0.016 nM dasatinib and graphed as a percentage of the uninhibited activity to determine dasatinib's IC_{50} : (•) WT = 3.5 nM; (\blacktriangle) Y395F = 9.0 nM.

Acknowledgments:

This research is based in part upon work conducted using the Rhode Island Genomics and Sequencing Center which is supported in part by the National Science Foundation under EPSCoR Grants Nos. 0554548 & EPS-1004057. We would also like to thank the lab of Niall Howlett for their expert advice on running western blots.

Works Cited:

- [1] N. Kohmura, T. Yagi, Y. Tomooka, M. Oyanagi, R. Kominami, N. Takeda, J. Chiba, Y. Ikawa, S. Aizawa, A novel nonreceptor tyrosine kinase, Srm: cloning and targeted disruption. *Mol Cell Biol* 14 (1994) 6915-6925.
- [2] Y. Kawachi, H. Nakauchi, F. Otsuka, Isolation of a cDNA encoding a tyrosine kinase expressed in murine skin. *Exp Dermatol* 6 (1997) 140-146.
- [3] K. Neet, T. Hunter, Vertebrate non-receptor protein-tyrosine kinase families. *Genes to cells : devoted to molecular & cellular mechanisms* 1 (1996) 147-169.
- [4] D.R. Robinson, Y.M. Wu, S.F. Lin, The protein tyrosine kinase family of the human genome. *Oncogene* 19 (2000) 5548-5557.
- [5] J.C. Darnell, K.B. Jensen, P. Jin, V. Brown, S.T. Warren, R.B. Darnell, Fragile X mental retardation protein targets G quartet mRNAs important for neuronal function. *Cell* 107 (2001) 489-499.
- [6] M.S. Serfas, A.L. Tyner, Brk, Srm, Frk, and Src42A form a distinct family of intracellular Src-like tyrosine kinases. *Oncology research* 13 (2003) 409-419.
- [7] J. Moffat, D.A. Grueneberg, X. Yang, S.Y. Kim, A.M. Klopfer, G. Hinkle, B. Piqani, T.M. Eisenhaure, B. Luo, J.K. Grenier, A.E. Carpenter, S.Y. Foo, S.A. Stewart, B.R. Stockwell, N. Hacohen, W.C. Hahn, E.S. Lander, D.M. Sabatini, D.E. Root, A lentiviral RNAi library for human and mouse genes applied to an arrayed viral high-content screen. *Cell* 124 (2006) 1283-1298.
- [8] T. Kubo, Y. Kuroda, H. Shimizu, A. Kokubu, N. Okada, F. Hosoda, Y. Arai, Y. Nakamura, H. Taniguchi, K. Yanagihara, I. Imoto, J. Inazawa, S. Hirohashi, T. Shibata, Resequencing and copy number analysis of the human tyrosine kinase gene family in poorly differentiated gastric cancer. *Carcinogenesis* 30 (2009) 1857-1864.

- [9] J.H. Ostrander, A.R. Daniel, C.A. Lange, Brk/PTK6 signaling in normal and cancer cell models. *Current opinion in pharmacology* 10 (2010) 662-669.
- [10] P.M. Brauer, A.L. Tyner, RAKing in AKT: a tumor suppressor function for the intracellular tyrosine kinase FRK. *Cell cycle* 8 (2009) 2728-2732.
- [11] P.M. Brauer, A.L. Tyner, Building a better understanding of the intracellular tyrosine kinase PTK6 - BRK by BRK. *Biochimica et biophysica acta* 1806 (2010) 66-73.
- [12] R. Roskoski, Jr., Src kinase regulation by phosphorylation and dephosphorylation. *Biochem Biophys Res Commun* 331 (2005) 1-14.
- [13] D.J. Kemble, Y.H. Wang, G. Sun, Bacterial expression and characterization of catalytic loop mutants of SRC protein tyrosine kinase. *Biochemistry* 45 (2006) 14749-14754.
- [14] K. Huang, Y.H. Wang, A. Brown, G. Sun, Identification of N-terminal lobe motifs that determine the kinase activity of the catalytic domains and regulatory strategies of Src and Csk protein tyrosine kinases. *J Mol Biol* 386 (2009) 1066-1077.
- [15] F.W. Studier, Protein production by auto-induction in high density shaking cultures. *Protein expression and purification* 41 (2005) 207-234.
- [16] A. Nasrolahi Shirazi, R.K. Tiwari, A. Brown, D. Mandal, G. Sun, K. Parang, Cyclic peptides containing tryptophan and arginine as Src kinase inhibitors. *Bioorg Med Chem Lett* 23 (2013) 3230-3234.
- [17] Y.H. Wang, M.K. Ayrappetov, X. Lin, G. Sun, A new strategy to produce active human Src from bacteria for biochemical study of its regulation. *Biochem Biophys Res Commun* 346 (2006) 606-611.
- [18] R.E. Joseph, A.H. Andreotti, Bacterial expression and purification of interleukin-2 tyrosine kinase: single step separation of the chaperonin impurity. *Protein expression and purification* 60 (2008) 194-197.

- [19] G.L. Rosano, E.A. Ceccarelli, Rare codon content affects the solubility of recombinant proteins in a codon bias-adjusted *Escherichia coli* strain. *Microbial cell factories* 8 (2009) 41.
- [20] M. Seto, T. Ogawa, K. Kodama, K. Muramoto, Y. Kanayama, Y. Sakai, T. Chijiwa, M. Ohno, A novel recombinant system for functional expression of myonecrotic snake phospholipase A(2) in *Escherichia coli* using a new fusion affinity tag. *Protein expression and purification* 58 (2008) 194-202.
- [21] C.W. Dessauer, S.G. Bartlett, Identification of a chaperonin binding site in a chloroplast precursor protein. *J Biol Chem* 269 (1994) 19766-19776.
- [22] J. Martin, T. Langer, R. Boteva, A. Schramel, A.L. Horwich, F.U. Hartl, Chaperonin-mediated protein folding at the surface of groEL through a 'molten globule'-like intermediate. *Nature* 352 (1991) 36-42.
- [23] J.S. Tokarski, J.A. Newitt, C.Y. Chang, J.D. Cheng, M. Wittekind, S.E. Kiefer, K. Kish, F.Y. Lee, R. Borzilleri, L.J. Lombardo, D. Xie, Y. Zhang, H.E. Klei, The structure of Dasatinib (BMS-354825) bound to activated ABL kinase domain elucidates its inhibitory activity against imatinib-resistant ABL mutants. *Cancer Res* 66 (2006) 5790-5797.
- [24] N. Vajpai, A. Strauss, G. Fendrich, S.W. Cowan-Jacob, P.W. Manley, S. Grzesiek, W. Jahnke, Solution conformations and dynamics of ABL kinase-inhibitor complexes determined by NMR substantiate the different binding modes of imatinib/nilotinib and dasatinib. *J Biol Chem* 283 (2008) 18292-18302.

MANUSCRIPT 2

Prepared for submission to the Journal of Medicinal Chemistry

***Design, synthesis and evaluation of dasatinib-derived protein-tyrosine kinase
inhibitors***

Alex Brown¹, Rakesh Tiwari², Amir Nasrolani Shirazi², Jarod Bolton², Keykavous Parang², Gongqin Sun^{1*}

*(1) Department of Cell & Molecular Biology, and (2) Department of Biomedical and Pharmaceutical Sciences, University of Rhode Island, 120 Flagg Road, Kingston, RI 02881. *gsun@uri.edu*

Abstract

Kinase inhibitors frequently suffer from a lack of specificity, most likely due to the high degree of conservation within their targets' ATP binding pockets. We reasoned that specificity may be developed by extending the inhibitor out from the traditional binding pocket to interact with more diverse sites. To test this hypothesis, derivatives of dasatinib were synthesized via esterification with one of 25 small molecules, thereby increasing the chemical diversity of the kinase inhibitor. Our approach generated numerous inhibitory compounds with enhanced kinase selectivity. Moreover, several unique characteristics of these inhibitors were explored for their potential utility as pro-drugs or research tools. Together, these findings highlight the great potential for this novel strategy with broad applications for the design and development of kinase-specific inhibitors.

Introduction

Protein tyrosine kinases (PTKs) are involved in numerous pathologies, including many cancers. Subsequently, PTK inhibitors have proven to be invaluable research and therapeutic tools. Current PTK inhibitors are mostly ATP analogs and are quite limited with regard to their specificity.¹ Ideally, such molecules would be able to target the aberrant kinases without interfering with normal physiological kinase signaling. This problem stems from a lack of structural diversity in the ATP/inhibitor binding pocket, similar in all kinases. The potent tyrosine kinase inhibitor (TKI) dasatinib (BMS-354825) is a case in point. It binds to the ATP binding site of many PTKs and is a potent, broad spectrum PTK inhibitor.²

The discovery and development of dasatinib was announced by Bristol-Myers Squibb in 2004 as an orally administered anticancer compound.³ In 2006, the company was granted tentative FDA approval for dasatinib, via the accelerated review process, and began marketing the drug as Sprycel®.⁴ Initially, approved indications for use applied only to adult patients diagnosed with either Philadelphia chromosome-positive (Ph+) chronic myeloid leukemia (CML) in the chronic phase, or Ph+ acute lymphoblastic leukemia (ALL), who were intolerant or resistant to standard imatinib (Gleevec, by Novartis) treatment. In 2010, full approval was granted for the treatment of imatinib resistant Ph+ ALL/CML, once further safety and efficacy was established. This extended the approved indications to include less developed Ph+ CML, still in the accelerated or blast phases.⁵

The Ph+ profile of many ALL/CML cancers is readily observed via standard karyotype, as it involves a specific translocation between chromosomes 9 and 22.⁶ This chromosomal aberration induces abnormal expression of a BCR-Abl fusion-protein. The fusion of the two proteins disrupts the normal regulatory mechanisms of each. In particular, the loss of the N-terminal domains of Abl removes key components of substrate recognition, cellular localization, and catalytic inactivation. The truncated kinase is responsible for creating a highly distorted pattern of phosphorylation, upsetting normal cell signaling dynamics, and leading to the oncogenic progression of ALL or CML. TKIs, such as imatinib and dasatinib, inhibit cancer progression by blocking the kinase activities of BCR-Abl and/or other kinases that are known to contribute oncogenic signaling, such as Src Family Kinases (SFK).

Dasatinib inhibits SFKs, BCR-Abl, c-KIT, EphA2, PDGFR-beta kinases with nanomolar or sub-nanomolar IC₅₀.⁵ It has been also crystalized as a bound ligand to the Abl, BMX, BTK, EphA4, Lyn, p38alpha, p38MAP, and Src kinases.⁷⁻¹⁴ The common manner in which it binds to each of these kinases, suggests it should be similar for many other kinases, too. This may, in part, explain side-effects of the compound at clinical dosage. Moreover, the clinical dosage, itself, may be limited by toxicity due to off-target kinase inhibition. This can lead to the persistence of cancer in small, drug-resistant populations and, ultimately relapse of patients who were previously in remission. In some patients, mutations arise during the course or treatment, or before. In all of these cases, where resistance has developed, alternative therapies must be sought.

These problems associated with balancing toxicity with effective dosage are not unique to dasatinib. All currently available TKIs are expected to lose effectiveness at some point to restart disease progression. From this perspective, it seems obvious that greater kinase specificity should be a top priority in the development of novel therapeutic inhibitors. However, it seems likely that many kinases share too great a degree of similarity to reasonably expect true specificity from ATP analogs, even from drugs with the potency of a molecule like dasatinib.

Outside of the ATP binding cleft of PTKs there are several regions of great variability amongst kinases, as demonstrated in Figure 1. Outside of the kinase's active site and lacking a defined binding pocket, these regions have garnered little attention as drug targets, on their own. However, by extending inhibitors from the ATP binding pocket into nearby variable regions, inhibitors may obtain greater capacity for specificity, through new interactions, while maintaining much of their affinity via ATP binding cleft interaction. Conveniently, certain PTK inhibitors, including dasatinib, bind to the kinase in such a way that a small portion of the molecule resides just outside of the ATP binding cleft. It has been demonstrated previously that chemical modifications to these drugs can be made to this position to facilitate attachment of chromatographic resins for affinity purification.¹⁵⁻¹⁷ By addition of small molecules to the dasatinib scaffold, it may be possible to extend the binding site to include regions of the kinase that are more diverse in order to impart greater potential PTK specificity.

We sought to evaluate this strategy by linking dasatinib to a series of small molecule adducts via esterification reactions. Following favorable molecular modeling results, we employed this technique to build a small library of 26 compounds (Figure 2). A diverse panel of non-receptor PTKs (including Csk, Abl, and Src) served as a basis for evaluating these compounds in terms of their potency and specificity. Several selected compounds were then further explored to reveal some unique properties and potential applications of these novel inhibitors.

Figure 1.

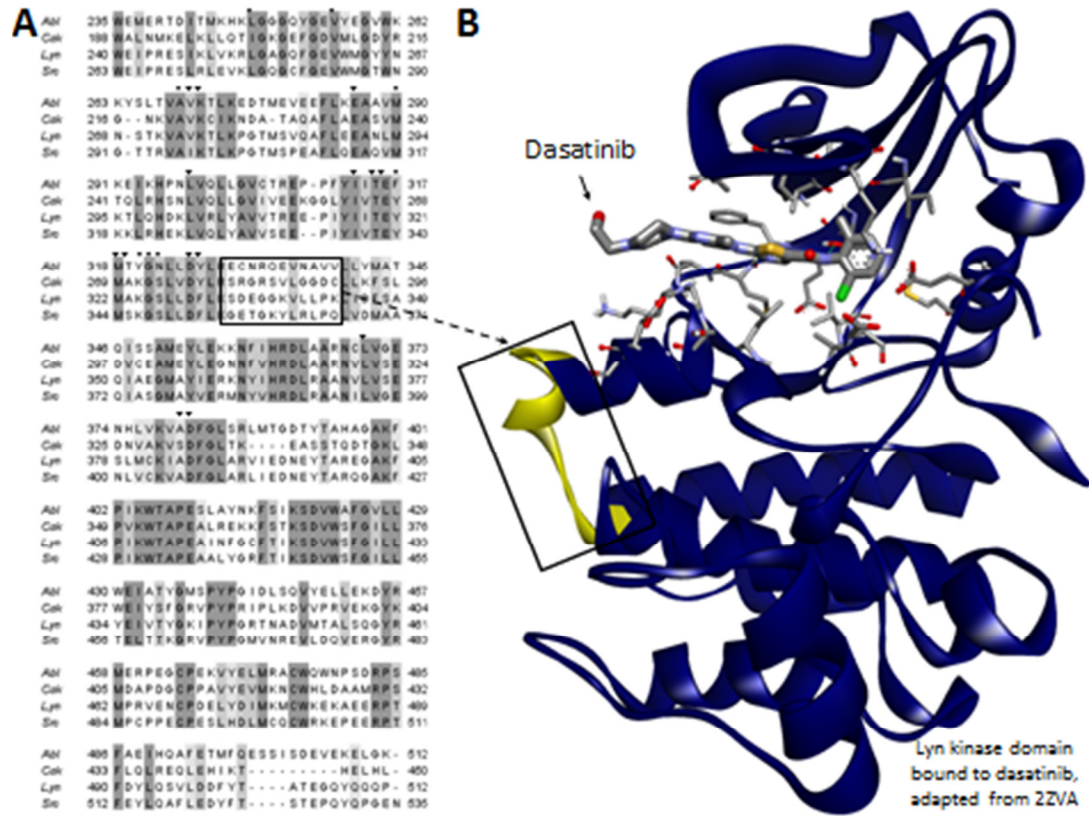


Figure 1. Structural elements of inhibition. Dasatinib inhibition of kinase activity is mediated by molecular interaction with highly conserved residues from the ATP-binding cleft of the catalytic domain. **(A)** The MUSCLE aligned protein sequences from the catalytic domains of Abl, Csk, Src, and Lyn illustrate the level of conservation throughout various regions of the catalytic domain among these diverse PTKs. The darker shaded portions of the alignment indicate greater conservation. The ligand-bound crystal structure of Lyn **(B)** demonstrates how dasatinib is docked within the catalytic domain. The inhibition of kinase activity is achieved via molecular interaction with amino acids of the ATP-binding cleft. These residues are displayed in stick form in the structure and also indicated by black arrowheads within the alignment. The region of the catalytic domain between the end of α -helix D and the beginning of α -helix E is boxed within the alignment and structure to highlight its inherent variability and proximity to the dasatinib binding site.

Figure 2.

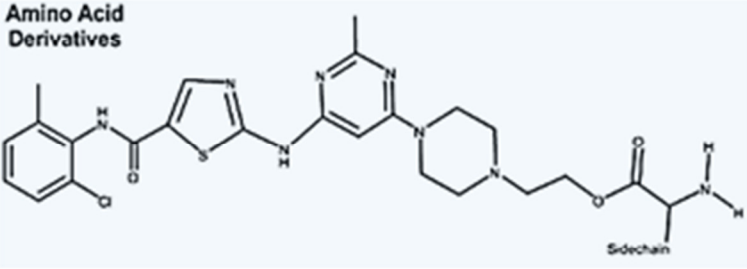
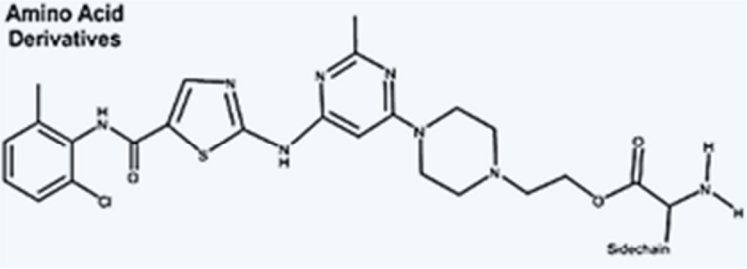
#	Compound	Structure
1	Dasatinib	
2	-G	<p>Amino Acid Derivatives</p> 
3	-βA	
4	-I	
5	-H	
6	-N	
7	-R	
8	-Q	
9	-W	
10	-L	
11	-Y	
12	-S	
13	-C	
14	-M	
15	-E	
16	-C ₂	
17	-C ₃	
18	-C ₁₀	
19	-C ₁₂	
20	-C ₁₄	
21	-C ₁₆	
22	-C ₁₈	
23	-C ₂₀	
24	-C ₁₁ -NH ₂	
25	-C ₁₂ -S-C ₂	
26	-G-Fluorescein	

Figure 2. Dasatinib derivatives. Dasatinib free-base (LC laboratories) was used as a scaffold for the attachment of various small molecules.

Results

Modeling

In order to establish the theoretical feasibility of binding and rule out any obvious steric hindrance, selected dasatinib derivatives were modeled and docked into the crystal structure of a PTK. The Lyn kinase (PDB code: 2ZVA) was chosen as it is a member of the clinically relevant SFKs.¹⁰ 2ZVA is a particularly good candidate among SFKs because it is nearly complete with few gaps and very good resolution. The resolution and completeness of this structure outside of the dasatinib binding pocket was essential, given that the additions to the core compound would potentially interact with a region outside the traditional binding pocket. Kinase catalytic domains are known to adopt at least two distinct conformations within crystal structures, active or inactive. To ensure that the proper conformation was used in docking studies, the structure (already bound by dasatinib) was edited to remove the co-crystallized ligand before modeling the compounds. In this manner, the parent compound could serve as a reference and control to ensure docking parameters were functioning properly.

We modeled each of the 20 common amino acids, along with addition of phosphotyrosine, as carboxyesters of dasatinib to establish the feasibility of our approach. This small collection of potential derivatives could be conveniently synthesized and represent of a variety of sizes and physical properties, while keeping computational cost low (by virtue of few rotatable bonds to calculate). Combining

accuracy and ease of use, we chose Autodock Vina to perform our *in silico* modeling. Autodock Vina's performance in docking has been relatively well established and its algorithms require no assumptions to be made concerning the ionization of side-chains.^{18, 19}

All of the compounds were docked and the top conformational hits of each were scored and ranked by the calculated binding energies that were reported in the program's docking summaries (Figure 3). The reference control, dasatinib, showed little deviation from the original crystallized ligand when its coordinates were superimposed. Additionally, the core dasatinib portion of each derivative was also nearly identical. We calculated a K_D of 8.3nM from the binding energy of -10.9 kcal/mol, which is in good agreement with the experimentally determined value of 3nM by our later assays. The calculated binding energies of all derivatives are within 0.9 kcal/mol of the dasatinib control.

The favorable binding energies of the docking simulations helped to support the notion that small molecules would not likely prohibit dasatinib binding when linked via esterification. These adducts were predicted to extend out from the ATP binding pocket with little, if any, disturbance to the normal mode of dasatinib binding. Furthermore, the favorable increases in calculated affinity in some dockings suggested that some small molecules could favorably interact with portions of the kinase, outside the ATP binding pocket.

Figure 3.

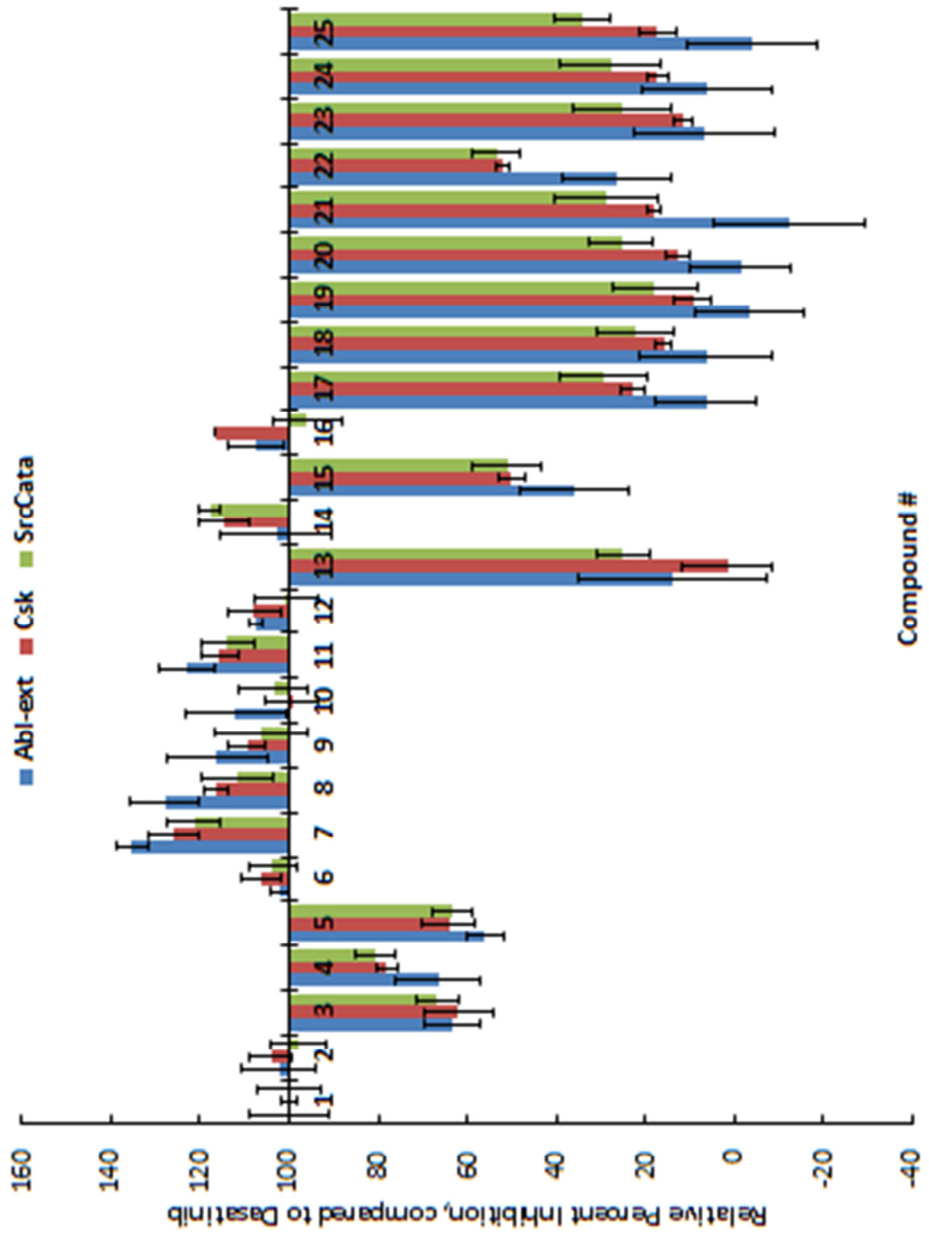


Figure 3. Inhibitor screening results. Results of screening of compounds at a fixed concentration against each of the panel PTKs. The activity of uninhibited enzyme was compared to dasatinib-inhibited enzyme activity to establish a baseline of inhibition. Each of the compounds were then compared to dasatinib inhibition for each enzyme. Bars above the x-axis show increased potency, while those below indicate a decreased capacity to inhibit the kinase, relative to dasatinib.

Design and Synthesis

Encouraged by the docking studies, we derivatized dasatinib by chemical esterification with various amino acids (for reasons stated above) using the protocols detailed in the methods section. Alongside these compounds, additional derivatives were synthesized by esterification with several fatty acids. These particular derivatives were chosen to evaluate their potential use as linkers to sites more distal to the ATP binding pocket. From this approach, 25 compounds were successfully synthesized and purified including 14 amino acid and 10 fatty acid adducts of dasatinib (Compounds 2-25). Compound 26 was later synthesized as a fluorescein-glycine ester to further demonstrate the utility of such chemical derivatives. Synthesis yields were good, overall, ranging from 70-95%.

Compound Screening

Each of the amino acid and fatty acid inhibitors were screened at a fixed concentration against Abl, Csk, and Src PTKs. Their percent inhibition relative to dasatinib was then determined. The results of this screening (Figure 3) offered insight as to the potency of each adduct, relative to dasatinib. Moreover, this relative profile could be compared between Abl, Csk, and Src kinases. Thus, this screening helped to highlight potential patterns of enhanced or diminished inhibition relating to the type of adduct.

In general, fatty acid-derived compounds dramatically decreased inhibitor potency. Of these compounds, only 16 (-C₂) inhibited comparably to dasatinib. Each of the remaining derivatives achieved less than 60% of dasatinib's inhibition toward each kinase. The screening profile of compound 24 (-C₁₁NH₂), when compared to that of similarly sized compounds (-C₁₀, -C₁₂, and -C₁₁SC₂), suggests that hydrophobicity, not size, accounts for much of these inhibitors' reduced potency. Furthermore, losses in potency due to long, hydrophobic chains may be recovered, at least in part, by linkage to a polar functional group (like -NH₂).

The amino acid derived compounds showed significantly greater potency over fatty acyl derivatives, with the exception of compound 13 (-C). Compound 15 (-E) also displayed a significantly reduced potency when compared to other amino acid derivatives. Compound 7 (-R) appeared to be the most potent of the inhibitors tested against all three kinases. We scrutinized docking results to identify a plausible explanation for this apparent increase in potency. Interestingly, the side-chain guanidium group of compound 7 (-R) was predicted to form a hydrogen bond with the backbone of the kinase, just outside the ATP binding-cleft.

The major changes in potency by our derivatives are interesting and perhaps informative, but are not the main focus of our study. Since we endeavor to isolate an active agent with altered kinase selectivity, the compounds' variable potency between kinases was our greatest concern. Compounds 21 (-C₁₆), 24 (-C₁₁NH₂), and 23 (-C₂₀) showed a significantly decreased capacity to inhibit Abl, as compared to the

other kinases. Compound 7 (-R), however, demonstrated its potency gains were greatest for Abl. Additionally, compound 16 (-C₂) displayed significantly increased potency toward Csk when compared to Abl and Src. The screening assay's sensitivity, however, limited the extraction of further selectivity results.

IC₅₀ determination

The screening, while relatively rapid, is not particularly sensitive and, thus, is limited in the task of identifying changes in kinase specificity. We further characterized the inhibition of selected compounds via IC₅₀ assays toward each of the kinases. First, compound 7 (-R) was chosen because it was one of the best compounds screened for each of the kinases in terms of potency and selectivity. We then chose compounds 3, 13, and 15 (-A, -C, -E) to use as a basis for comparison and to tease out potential differences in selectivity. For the fatty acid-derived compounds, we again chose to compare the most potent compound, 16 (-C₂), one longer chained derivative (21, -C₁₆), two moderately long-chained compounds (17/-C₈, 18/-C₁₀), and the potential linker compound 24 (-C₁₁NH₂) for further investigation.

The results of the IC₅₀ assays, summarized in Table 1, reflect the potency of the compounds toward each of the PTKs. As predicted by the screenings, compound 7 (-R) displayed increased potency against all kinases with an average 37% decrease in IC₅₀ compared to dasatinib. The greatest gain in potency was observed for Abl by

compound 7 (-R) with an IC_{50} of 0.45nM as compared to the 0.75nM value for dasatinib, representing a 42% decrease. Conversely, compound 13 (-C) was the worst performing of the amino acid derivatives with IC_{50} 's ranging from 1.7 - 5.3x higher than dasatinib toward our PTK panel. Interestingly, compound 15 (-E) performed about as well as compound 3 (-A), despite the latter showing possible signs of greater potency in the screenings.

To garner more quantitative insight into potential gains or losses in enzyme selectivity, the IC_{50} of each compound toward a particular kinase can be compared to the IC_{50} of the same compound for another kinase, in the form of a ratio. For example, the IC_{50} of dasatinib is 7nM for Csk and 0.37nM for Src, giving a C/S ratio of 18.9, clearly indicating specificity toward Src. When comparing Abl and Src, however, a A/S ratio of 2.1 for dasatinib implies that the compound inhibits both kinases in rather non-selective fashion. In this manner, ratios greater than 10 or less than 0.1 reflect IC_{50} 's that differ by more than an order of magnitude, and the inhibitor is generally considered to be selective or specific for the kinase with the lower IC_{50} .

Comparisons of the specificities for each of the compounds toward Csk shows that two compounds, 7 (-R) and 16 (-C₂), showed little change in their preference for Src (17.6 A/S and 16.7 C/S, respectively). However, each of the remaining compounds increased their preference for Src dramatically with C/S IC_{50} ratios of 30.0 or higher. The highest selectivity ratio obtained in our study, 91.4 C/S, was from this group and belonged to compound 18 (-C₁₀) with an IC_{50} for Csk = 3.2 μ M compared to

35nM for Src. This marks a difference of almost two orders of magnitude between the IC₅₀ values. Additionally, each of these compounds displayed increased selectivity toward Src, as compared with Abl. Of particular note, compound 15 (-E) and compound 13 (-C) demonstrated the largest gains (10.2 and 10.3 A/S IC₅₀ ratios). These two dasatinib derivatives represent the only bona-fide Src specific inhibitors in our dataset, as they possess IC₅₀'s at least an order of magnitude higher for both Abl and Csk, and present a significant increase in kinase specificity when compared to dasatinib.

Table 1.

Inhibitor	IC50, nM			Selectivity			Net change in IC50(%Dasatinib)			
	Abl	Csk	Src	C/A	C/S	A/S	Abl	Csk	Src	Avg
Dasatinib	0.78	7	0.37	9.0	18.9	2.1	--	--	--	--
-R	0.45	4.4	0.25	9.8	17.6	1.8	-42	-37	-32	-37
-C2	2.1	5.5	0.33	2.6	16.7	6.4	169	-21	-11	46
-A	3	21	0.39	7.0	53.8	7.7	285	200	5	163
-E	4.4	20	0.43	4.5	46.5	10.2	464	186	16	222
-C11NH2	4.9	30	1	6.1	30.0	4.9	528	329	170	342
-C	68	500	6.6	7.4	75.8	10.3	8618	7043	1684	5782
-C8	51	600	7.5	11.8	80.0	6.8	6438	8471	1927	5612
-C10	220	3200	35	14.5	91.4	6.3	28105	45614	9359	27693
-C16	680	5100	75	7.5	68.0	9.1	87079	72757	20170	60002

Table 1. Summary of inhibitor potency and selectivity. Selected compounds were evaluated against each of the enzymes in our panel. Potency was measured via IC_{50} in standard P32 kinase assay with appropriate substrate. Selectivity is represented as the ratio of IC_{50} for one enzyme over another. The change in IC_{50} , as compared to dasatinib, is calculated and shown in the right-most columns to illustrate how potency was effected.

Assaying the dynamic nature of dasatinib esters

Given the profound influence of drug metabolism on inhibitor efficacy, we characterized how our synthesis strategy may impart a unique and favorable metabolic profile. *In vivo*, numerous carboxyesterases have been shown to hydrolyze ester bonds of compounds (similar to those in the dasatinib derivatives), particularly upon circulation to the liver. Mouse microsomal preparations contain relatively high concentrations of carboxyesterases and frequently serve as proxies for the liver in drug metabolism studies. In a variation of our kinase assay, select compounds were pre-treated with these microsomal preparations prior to assaying for kinase inhibition, alongside the untreated compound. If the derivative is a suitable substrate for one or more carboxyesterase, the products of the subsequent reaction should include the core dasatinib molecule. The assays relied upon the careful consideration of proper compound concentration and a significant difference in potency between the derivative and dasatinib. Executed properly, the microsomal esterase activity toward the compound in question can be monitored as a function of kinase inhibition.

As the dasatinib derivatives vary substantially in size and chemical properties, it is worth noting that stability of the derivative likely fluctuates between compounds, according to variations in substrate specificities of carboxyesterases. With this dynamic in mind, we chose representative compounds for the assays, namely *13* (-C) and *17* (-C₈). From the results, summarized in Figure 4, it appears that

compound *13* (-C) is remarkably unaffected by carboxyesterases, even after 4 hours pre-treatment. The stability of this compound is in sharp contrast to that of *17* (-C₈), which showed significant changes in inhibition after just 20 minutes pre-treatment. After two hours, compound *17* (-C₈) inhibited nearly all kinase activity. This observation is consistent with adduct hydrolysis by microsomal carboxyesterase and recovery of the dasatinib core molecule (which is more than six times as potent). The dynamic offered by these esterified derivatives can be quite advantageously applied toward engineering a unique drug metabolic profile.

Figure 4.

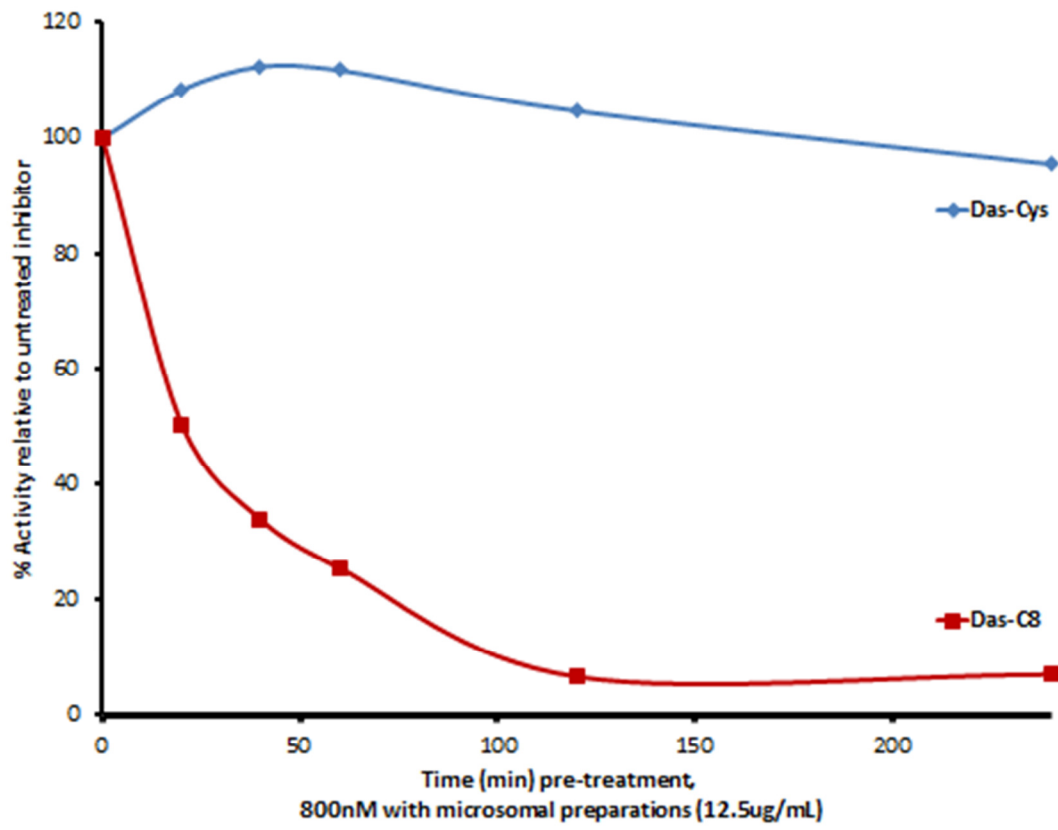


Figure 4. Microsomal preparations metabolize dasatinib derivatives. Treatment of compounds with mouse microsomal preparations prior to inhibition assays demonstrate the differential metabolism of compounds, likely due to deesterification via carboxyesterases. The time course was done with compounds -C and -C8 at 800nM against Abl to highlight the differences. At this concentration, each compound is expected to have little to no inhibition of Abl as a result of the adduct used at the derivatized position of dasatinib. After 2 hours of treatment, compound -C₈, but not -C, recovers almost all of its potency, relative to the core compound.

Development of a fluorescent dasatinib derivative

To expand upon the vast potential offered by dasatinib derivatives, we sought to construct a fluorescent probe for *in vitro* characterization of kinases. Tethered to dasatinib by a glycine linker, a fluorescein conjugated derivative was synthesized (compound 26). The compound was assayed against Src, finding an IC_{50} of 1nM. The affinity of the dasatinib-fluorescein compound was then measured using a fluorescence polarization binding assay.

In such an assay, polarized light of a specific wavelength is used to excite the fluorescein molecule, which in turn emits light at a higher wavelength. The degree to which the emitted light is depolarized depends on the free rotation of fluorescein, which is inversely correlated with ligand binding. Thus, the binding affinity of a fluorescein-ligand conjugate for a given receptor can be measured by recording the polarization of light in serial dilution of the receptor and fitting the data to a standard ligand binding curve.

We sought to measure the affinity of our ligand for a form of Src that is deficient in kinase activity (kdSrc). This mutant kinase is often able to be purified to significantly higher concentrations than active kinase, which adds to the convenience of the assay and broadens its potential application (as discussed later). The binding curve generated from these assays (shown in Figure 5A) reveals an affinity of 15nM toward kdSrc by our fluorescein-dasatinib conjugate (compound 26). This value was

higher than expected and may reflect differences between active/inactive kinase forms or limitations of the assay's lowest detection limit.

To explore the utility of this fluorescent probe, we employed a variation of this assay to determine the binding affinity of unlabeled dasatinib via a competitive binding assay. In this assay, fixed concentrations of the fluorescent probe and kinase were used to produce a high polarization signal. The reactions were then titrated with unlabeled dasatinib while recording polarization. The resulting data was graphed and curve fitting analysis provided a binding constant of 3nM for dasatinib (Figure 5B).

The results of these fluorescence polarization binding assays with kinase deficient substrate are fairly consistent with the IC_{50} 's derived from the radio-ligand kinase assays. The difference between the measured affinities of the fluorescent probe and dasatinib accurately predict the relative potency of the compounds as kinase inhibitors. Combined with the ease of polarization binding assays, the utility of compound 26 (-G-Flu) as a probe for inhibitor development is clear.

Figure 5.

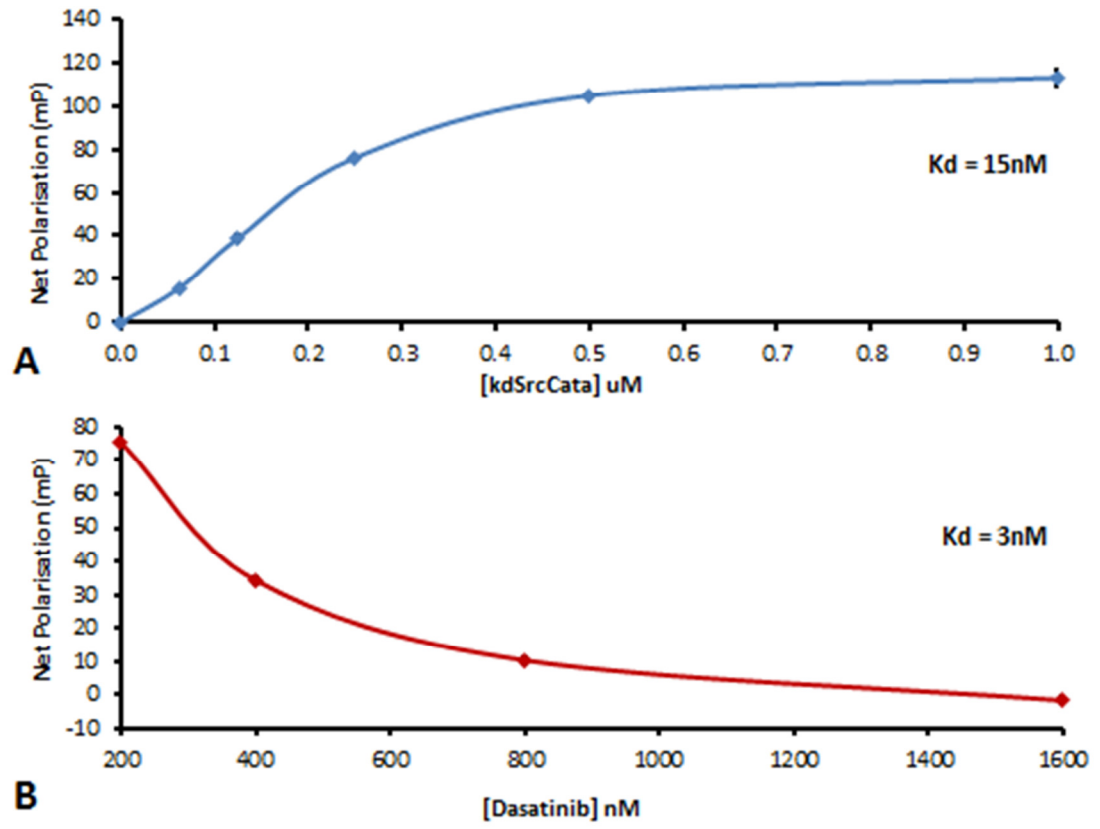


Figure 5. Polarization binding assays using a fluorescent dasatinib derivative. **(A)** Fluorescence polarization assay of the kinase deficient Src catalytic domain titrated against compound -G-Flu (400nM). A K_d of 15nM was determined for the ligand. **(B)** Competitive binding assay of compound -G-Flu (50nM) and dasatinib against the kinase deficient Src catalytic domain (125nM) reveals a K_d of 3nM, as measured via fluorescence polarization (50mM HEPES, pH 8.0).

Discussion and Conclusions

Library construction

Based upon the wealth of available structural data and past successes of dasatinib modifications for affinity-based interaction studies, we hypothesized that the exceptional potency of dasatinib would support its use as a molecular scaffold for the synthesis of novel kinase inhibitors with enhanced specificity. The solved crystal structures of dasatinib in complex with several PTK catalytic domains demonstrate the common manner in which the inhibitor binds PTK active sites. Particularly intriguing to us, is a hydroxyl group of dasatinib that extrudes from the binding pocket to the surface of the kinase. In literature, there are numerous examples of dasatinib (and other kinase inhibitors, as well) that have been modified at this position through the coupling of compounds to agarose resin or other molecules. These modifications enabled efficient extraction of PTKs that are potential dasatinib targets from various cancer cells and tissues. These affinity-driven applications rely upon specific interaction or recognition of kinases, which suggests that the inhibitor portions of these compounds retain, at least in part, their ability to bind PTK active sites. We reasoned that if large resin attachment does not abolish the affinity of dasatinib, then smaller chemical adducts should be well tolerated, too.

In the present study, we sought to take advantage of this feature of dasatinib by attaching a series of small molecules in an effort to impart novel inhibitor characteristics. In the spirit of rapid library development, we desired a synthesis

strategy that was efficient, convenient, and easily employed to obtain derivatives with a wide range of chemical properties. To meet these criteria, we opted for batch synthesis directly from dasatinib (free base) by esterification of its hydroxyl group to carboxylic acid containing compounds.

A potential drawback to any derivitization, of course, is the potential destruction of key features of the original molecule. During initial development of dasatinib by Bristol-Meyers-Squibb, the hydroxyl group was determined to be necessary for proper activity of the inhibitor (personal communication with R. Tiwari, addition citation?). Upon review of the crystallized ligand, it seems likely that the proper binding orientation of the core molecule is stabilized by energetically favoring exclusion of the alcohol from the binding pocket. Docking studies of this molecule without the hydroxyl group support this idea, as calculated binding energies rise and predicted conformation deviates substantially from the known crystal structures. Additionally, this polar group's inclusion probably enhances the solubility or bioavailability of hydrophobic dasatinib core molecule. Thus, our derivitization of dasatinib, which targets this position for modification, threatens to disturb proper binding conformation and solubility-related characteristics. The potency with which the derivatives inhibit the PTKs in our panel suggests proper orientation is likely achieved by most, if not all compounds.

Derivatization alters kinase selectivity

The structural diversity of target kinases is a central element to this study, as we endeavor to identify the different types of inhibitor interactions that confer specificity. For this reason, we chose three kinases that represent divergent non-receptor PTK families, distinct in structure and function. An ideal inhibitor would target just one of these kinases through recognition of one or more of its distinct structural features, not found in more distantly related PTKs. Therefore, our diverse panel of kinases serves to increase our chances of identifying novel compounds that more closely resemble an ideal inhibitor.

With that idea in mind, it is important to recognize that our kinase inhibitor scaffold, dasatinib, already has a built in bias toward certain kinases, particularly the Abl and Src families, as compared to others, like Csk. This suggests two things: first, that dasatinib recognizes structural elements common to all three kinases, and second, that Csk possesses features that limit this interaction. It is, therefore, reasonable to assume that complete reversal in this pattern of specificity is unlikely to occur without a major change in binding mode. The inhibitor would not only have to overcome its previously limited interaction with Csk, but also would have to develop some new interaction that is not tolerated by Abl and Src. Therefore, when starting from a biased inhibitor, altered selectivity is probably most likely to occur as a result of either the elimination or exaggeration of an inherent bias.

From this line of reasoning, it makes sense that our library of derivatives displays no signs of dramatic reversals in kinase selectivity pattern. All of the compounds investigated better inhibit Src than Abl, and Abl was always inhibited more than Csk. This apparent limitation aside, our measures of selectivity do change dramatically for a number of inhibitors, simply by enhancing a pre-existing bias of dasatinib for or against a given kinase. In one of the most dramatic examples, the IC_{50} of compound *15* (-E) increased only mildly for Src (+16%) but greatly for Csk (+186%) and even more so for Abl (+486%). While other compounds such as *13* (-C) and *18* (-C₁₀) also possessed significantly altered kinase selectivity, compound *15* (-E) was particularly unique for its minimal loss of potency toward Src.

The changes in kinase inhibitor specificity are quite remarkable considering the limited size of the library generated. Compound *15* (-E) demonstrates the ease with which dasatinib derivatives can be developed to significantly alter kinase selectivity. An IC_{50} for Src that is more than a magnitude lower than for other kinases is certainly quite notable and, we believe, represents a major step in the development of truly specific PTK inhibitors. Furthermore, this success can be built upon by expanding this strategy to include many new dasatinib derivatives for study and comparison to compound *15* (-E).

Structural basis of increased selectivity

The structural variation of PTKs outside the ATP binding pocket is localized to a few small areas. One such region is located at the end of α -helix D of the peptide binding lobe and extends to α -helix E. Even among closely related PTKs, like the Src Family Kinases, a great deal of structural variation exists here. This region has also been implicated as a key site of substrate recognition in some kinases.²⁰ Furthermore, α -helix D is in very close proximity (within a few angstroms) to the hydroxyl group of dasatinib.

One hurdle to developing dasatinib derivatives in this manner has to do with the size of the compounds being tethered to the inhibitor. If these are too short or too long, they will likely miss the targeted α -helix D. Likewise, bulkier compounds threaten to interfere via steric hindrance. One means by which we sought to alleviate such concerns was to simulate the binding of potential compounds using molecular modeling software. Retrospective analysis of these models, in conjunction with our biochemical data and the available crystal structures of Abl, Csk, and Src, offer valuable insight into the changes in specificity we observed from our compounds.

The first and, perhaps, most exciting feature that the models predict is the preferred orientation of the compounds that were attached to dasatinib. Despite allowance to rotate freely, almost all of the simulated dockings favor interaction with the region surrounding α -helix D, rather than the equally proximal ATP binding lobe

of the kinase. Undoubtedly, this orientation better positions the inhibitor for possible contact with structural features that are unique to any given kinase.

For example, two of the three most common hydrogen bonds, uniquely formed by dasatinib derivatives, which we observed in the dockings, occur with side-chain residues of Lyn's α -helix D (S333 and E335). The corresponding sites of Src (G352 and M354) and Csk (S280 and R282) would clearly produce different results, while Abl deviates in structure so greatly at this position; it is hard to identify cognates. While it is difficult to make any specific claims from molecular docking simulations, it seems rather impossible to identify structural features other than α -helix D that could explain the level of differentiation that we observed, by the kinases we examined.

Key features of α -helix D may also explain the altered selectivity we observed of the fatty acid conjugated derivatives. The extreme effects that these molecules have on potency are likely due to exclusionary interactions with the polar surface of the kinase that surrounds the exit from the inhibitor binding pocket. This can easily be seen by coloring the surfaces of the kinases according to hydrophobicity. In Src, however, the pattern of hydrophobicity at the end region of α -helix D is such that a clear pathway to α -helix E (also fairly hydrophobic) is maintained. This may explain the longer-chained fatty acid derivatives' enhanced capacity to inhibit Src, relative to the other kinases.

The structural evidence examined thus far suggests that α -helix D offers the greatest potential avenue of interaction with the synthesized compounds. The novel specificities of the dasatinib derivatives we generated certainly imply unique interactions have been formed with the PTKs they inhibit. While more conclusive evidence remains to be collected, it appears highly likely that the modulation of kinase-specific inhibition observed in this study is a direct result of novel interactions outside the ATP binding pocket, particularly α -helix D.

Implications in drug metabolism

The ADME characteristics of a given kinase inhibitor are vital to its usefulness as a therapeutic tool. How well the drug gets taken into the target cells and how long it remains in active form are direct functions of the chemical properties inherent in the molecule. Particularly, susceptibility of a drug to the hosts' metabolic processes is a major part of this. The stability assays performed in this study highlight an important feature of our dasatinib derivatives.

Consider the compound *17* (-C₈), which displays a low nanomolar IC₅₀ that is over an order of magnitude greater than dasatinib. While this study does not address bioavailability, we have observed that the compound is readily metabolized to a highly active inhibitor by carboxyesterases from the liver. Therefore, if titrated properly, this compound may offer considerable value as a pro-drug for the extended release of dasatinib.

The utility of other derivatives, perhaps not metabolized by carboxyesterases, also opens the door for new applications. Compound 13 (-C) for example, is another low nanomolar inhibitor that actually displays enhanced specificity for Src compared to dasatinib. While overall potency is diminished to some degree, the added specificity may provide the proper trade-offs to enable more effective outcomes. Perhaps the most interesting feature of this compound, however, is its inability to be broken down by the microsomal preparations. The fact that the Cys adduct appears to disrupt the inhibitor's metabolic break-down offers evidence that this strategy may be employed to subvert other enzymatic components of a host's drug metabolism, to effectively increase half-life of the compound.

The broad applications offered by an altered drug metabolic profile are numerous and multifaceted. Any derivative, no matter how small the alteration, can potentiate major changes. The huge chemical diversity that is possible with the strategy we describe here, however, can be rapidly and conveniently applied to screen for desired characteristics, without resynthesizing the core dasatinib molecule. With these ideas in mind, further investigation of the unique ADME features of these compounds and newly synthesized dasatinib derivatives seems merited, given the potential therapeutic benefits of increased stability and extended release.

Fluorogenic dasatinib derivatives

Compound 26 (-G-Flu) is a dual-purpose inhibitor with broad potential applications. As an inhibitor, it can bind to a kinase tightly, while enabling its visible detection. This may be particularly useful as a molecular diagnostic tool for imaging. Likewise, *in vitro* techniques may find this compound useful in FACS for monitoring kinase expression. Since this compound is capable of measuring the binding of unlabeled inhibitor, it will be especially adaptable to high-throughput kinase inhibitor drug discovery.

Methods

Reagents and chemicals

[γ -³²P]-ATP (6,000 Ci mol⁻¹) was purchased from PerkinElmer for kinase assays and pre-cast protein gels were bought from BioRad. Dasatinib was obtained as free base from LC Laboratories. All reagents used for bacterial culture and protein expression were purchased from Fisher. All other chemicals reagents were obtained from Sigma.

Molecular Modeling

Crystal structure 2ZVA of protein-tyrosine kinase Lyn in complex with dasatinib (ligand identifier: 1N1) was downloaded from the PDB (www.pdb.org) and edited within AutoDockTools in preparation for simulations, according to the guidelines provided. In order to accurately reproduce the crystal structure in control dockings, the receptor was held rigid and the rotatable bonds (torsions) of the core dasatinib structure were frozen with the exception of the C13-N5 and N6-C20 bonds. Based on the superimposition of other solved structures, these appear to be the only bonds to display any great deviation from kinase-to-kinase. The virtual ligands were prepared using Discovery Studio (Dockings were performed with an exhaustiveness of 256 within a search space measuring 22x24x28, centered at (11, 90.5, 57.5) x,y,z.

Synthesis of Dasatinib Derivatives

Synthesis and purification of all dasatinib derivatives was carried out by the lab of Dr. Keykavous Parang, according to standard protocols.

Protein Expression and Purification

Enzymes and protein substrate were prepared as previously described.^{21, 22} Briefly, vectors for expressing Abl, CrkL, or Csk as GST-fusions and the 6xHis-tagged Src catalytic domain (SrcCata) were made and cloned into appropriate *E. coli* systems. For each, 1-liter LB cultures were grown at 37°C until an OD₆₀₀ of about 1 was reached and then induced at RT with 0.4 mM isopropyl β-d-thiogalactopyranoside while shaking at 250 rpm for 4-6 hours. Cells were harvested at 4°C via centrifugation at 7,000 x g. Pellets were either stored at -20°C or immediately re-suspended in appropriate lysis buffer: PBS + β-mercaptoethanol, pH 7.3 for GST-fusions and 50mM HEPES + 200mM NaCl + 10mM imidazole + 0.01% triton x-100, pH 8.0 for 6xHis-proteins. Following 4x15sec sonication in 12mL glass tubes on ice, lysates were cleared by centrifuge for 10min at 22,000 x g and incubated with 1mL agarose resin at 4°C for 1hr. This suspension was then loaded into a column, washed with lysis buffer and eluted with either 50mM Tris + 10mM GSH, for GST-fusions, or 50mM HEPES + 200mM imidazole to release 6xHis-tagged protein. All samples were quantified using standard Bradford assays and analyzed by SDS-PAGE/coomassie staining to check purity.

Kinase Assays and IC₅₀ Measurements

Enzyme activity and inhibition was characterized using the following methods, adapted from previous work.^{21, 22} Csk and SrcCata activity levels were measured from incubations with polyE₄Y (1mg/mL) and CrkL (0.5mg/mL) was used as a substrate for Abl. Dasatinib and derivatives were dissolved in 10% DMSO / 90% kinase buffer solution (KB10) and diluted in series as needed. In screening assay reactions, multiple inhibitors were used at a fixed concentration for relative inhibition comparisons. IC₅₀ measurement assays, however, had a single inhibitor but each reaction varied in the compound's concentration. In assays requiring pre-treatment, undiluted stocks of the inhibitors were incubated at RT with microsomal preparations to a final concentration of 12.5ug/mL.

In each assay, a series of 50μL duplicate reactions were setup at 30°C to contain the appropriate inhibitor concentration, substrate, and enzyme in 75mM EPPS, pH 8.0 + 200μM [γ-³²P]-ATP (~1000 dpm/pmol) + 12 mM MgCl₂ + 5% glycerol + 0.005% Triton X-100. The reactions were stopped after 20min incubation by blotting onto filter paper strips prior to precipitation and washing in hot 5% trichloroacetic acid. The strips were then sorted and separated into vials of scintillation fluid for signal quantification in a Beckman Coulter LS-6500. From these counts, enzyme turnover was calculated for each reaction.

Binding assays

To determine the binding of compound 26 (-G-Flu) toward the kinase-deficient Src catalytic domain (kdSrcCata), fluorescence polarization (FP) binding assays were carried out as described previously.^{23, 24} Specifically, a series of kdSrcCata dilutions were made, ranging from 62.5 – 1,000nM (and an additional blank). Each dilution contained 400nM compound 26 (-G-Flu) in 50mM Tris, pH 8.0. FP was then detected using a PerkinElmer LS55 Luminescence Spectrophotometer at 25°C. Wavelengths utilized were 485 nM for excitation and 530 nM for emission. The net change in FP was plotted as a function of kdSrcCata concentration and fit to the following equation: $FP = FP_{max} \times [kdSrcCata] / (K_D + [kdSrcCata])$. Where FP_{max} is the maximum polarization value at saturation and K_D is the dissociation constant of compound 26 (-G-Flu) binding to kdSrcCata. Regression analysis was carried out in LabFit software (www.labfit.net).

To determine the binding of unlabeled dasatinib, its ability to compete against the fluorogenic compound for binding to kdSrcCata was determined by an FP competition binding assay.²³ This assay setup differs from the above in that each tube had a 50nM concentration of compound 26 (-G-Flu), 125nM kdSrcCata (held constant), and concentrations of the unlabeled dasatinib from 200 – 1,600nM. The competing ligand's K_D was then determined by plotting the FP as a function of the increasing concentration of the unlabeled compound and fitting the curve to the equation: $FP = A \times ([kdSrcCata]_t \times [Probe]_t \times K_{D2}) / (K_{D1} \times K_{D2} + K_{D1} \times [Competitor]_t +$

$[kdSrcCata]_t \times K_{D2}$), where K_{D1} is the dissociation constant of compound 26 (-G-Flu), as determined above, and K_{D2} is the dissociation constant of the unlabeled dasatinib. A is a conversion factor between the concentration of the probe-kinase complex and the FP value. $[kdSrcCata]_t$ and $[Probe]_t$ were total kinase and compound 26 (-G-Flu) concentrations. $[Competitor]_t$ is the total concentration of unlabeled, competing ligand.

Works cited:

1. Zhang, J.; Yang, P. L.; Gray, N. S. Targeting cancer with small molecule kinase inhibitors. *Nature reviews. Cancer* **2009**, 9, 28-39.
2. Jilaveanu, L. B.; Zito, C. R.; Aziz, S. A.; Chakraborty, A.; Davies, M. A.; Camp, R. L.; Rimm, D. L.; Dudek, A.; Sznol, M.; Kluger, H. M. In vitro studies of dasatinib, its targets and predictors of sensitivity. *Pigment cell & melanoma research* **2011**, 24, 386-9.
3. Shah, N. P.; Tran, C.; Lee, F. Y.; Chen, P.; Norris, D.; Sawyers, C. L. Overriding imatinib resistance with a novel ABL kinase inhibitor. *Science* **2004**, 305, 399-401.
4. The FDA approves new leukemia drug; expands use of current drug. *FDA consumer* **2006**, 40, 5.
5. SPRYCEL[®] (dasatinib) [package insert]. In 2006 (REV 2012).
6. Liu-Dumlao, T.; Kantarjian, H.; Thomas, D. A.; O'Brien, S.; Ravandi, F. Philadelphia-positive acute lymphoblastic leukemia: current treatment options. *Curr Oncol Rep* **2012**, 14, 387-94.
7. Berman, H. M.; Westbrook, J.; Feng, Z.; Gilliland, G.; Bhat, T. N.; Weissig, H.; Shindyalov, I. N.; Bourne, P. E. The Protein Data Bank. *Nucleic Acids Res* **2000**, 28, 235-42.
8. Tokarski, J. S.; Newitt, J. A.; Chang, C. Y.; Cheng, J. D.; Wittekind, M.; Kiefer, S. E.; Kish, K.; Lee, F. Y.; Borzilleri, R.; Lombardo, L. J.; Xie, D.; Zhang, Y.; Klei, H. E. The structure of Dasatinib (BMS-354825) bound to activated ABL kinase domain

elucidates its inhibitory activity against imatinib-resistant ABL mutants. *Cancer Res* **2006**, 66, 5790-7.

9. Getlik, M.; Grütter, C.; Simard, J. R.; Klüter, S.; Rabiller, M.; Rode, H. B.; Robubi, A.; Rauh, D. Hybrid compound design to overcome the gatekeeper T338M mutation in cSrc. *J Med Chem* **2009**, 52, 3915-26.

10. Williams, N. K.; Lucet, I. S.; Klinken, S. P.; Ingley, E.; Rossjohn, J. Crystal structures of the Lyn protein tyrosine kinase domain in its Apo- and inhibitor-bound state. *J Biol Chem* **2009**, 284, 284-91.

11. Marcotte, D. J.; Liu, Y. T.; Arduini, R. M.; Hession, C. A.; Miatkowski, K.; Wildes, C. P.; Cullen, P. F.; Hong, V.; Hopkins, B. T.; Mertsching, E.; Jenkins, T. J.; Romanowski, M. J.; Baker, D. P.; Silvian, L. F. Structures of human Bruton's tyrosine kinase in active and inactive conformations suggest a mechanism of activation for TEC family kinases. *Protein Sci* **2010**, 19, 429-39.

12. Farenc, C.; Celie, P. H.; Tensen, C. P.; de Esch, I. J.; Siegal, G. Crystal structure of the EphA4 protein tyrosine kinase domain in the apo- and dasatinib-bound state. *FEBS Lett* **2011**, 585, 3593-9.

13. Muckelbauer, J.; Sack, J. S.; Ahmed, N.; Burke, J.; Chang, C. Y.; Gao, M.; Tino, J.; Xie, D.; Tebben, A. J. X-ray crystal structure of bone marrow kinase in the x chromosome: a Tec family kinase. *Chemical biology & drug design* **2011**, 78, 739-48.

14. Rothweiler, U.; Åberg, E.; Johnson, K. A.; Hansen, T. E.; Jørgensen, J. B.; Engh, R. A. p38 α MAP kinase dimers with swapped activation segments and a novel catalytic loop conformation. *J Mol Biol* **2011**, 411, 474-85.

15. Rix, U.; Hantschel, O.; Dürnberger, G.; Remsing Rix, L. L.; Planyavsky, M.; Fernbach, N. V.; Kaupe, I.; Bennett, K. L.; Valent, P.; Colinge, J.; Köcher, T.; Superti-Furga, G. Chemical proteomic profiles of the BCR-ABL inhibitors imatinib, nilotinib, and dasatinib reveal novel kinase and nonkinase targets. *Blood* **2007**, 110, 4055-63.
16. Zhou, G.; Sylvester, J. E.; Wu, D.; Veach, D. R.; Kron, S. J. A magnetic bead-based protein kinase assay with dual detection techniques. *Anal Biochem* **2011**, 408, 5-11.
17. Shi, H.; Zhang, C. J.; Chen, G. Y.; Yao, S. Q. Cell-based proteome profiling of potential dasatinib targets by use of affinity-based probes. *Journal of the American Chemical Society* **2012**, 134, 3001-14.
18. Trott, O.; Olson, A. J. AutoDock Vina: improving the speed and accuracy of docking with a new scoring function, efficient optimization, and multithreading. *J Comput Chem* **2010**, 31, 455-61.
19. Houston, D. R.; Walkinshaw, M. D. Consensus docking: improving the reliability of docking in a virtual screening context. *J Chem Inf Model* **2013**, 53, 384-90.
20. Lee, S.; Lin, X.; Nam, N. H.; Parang, K.; Sun, G. Determination of the substrate-docking site of protein tyrosine kinase C-terminal Src kinase. *Proc Natl Acad Sci U S A* **2003**, 100, 14707-12.
21. Huang, K.; Wang, Y. H.; Brown, A.; Sun, G. Identification of N-terminal lobe motifs that determine the kinase activity of the catalytic domains and regulatory strategies of Src and Csk protein tyrosine kinases. *J Mol Biol* **2009**, 386, 1066-77.

22. Kemble, D. J.; Wang, Y. H.; Sun, G. Bacterial expression and characterization of catalytic loop mutants of SRC protein tyrosine kinase. *Biochemistry* **2006**, 45, 14749-54.
23. Tiwari, R.; Brown, A.; Narramaneni, S.; Sun, G.; Parang, K. Synthesis and evaluation of conformationally constrained peptide analogues as the Src SH3 domain binding ligands. *Biochimie* **2010**, 92, 1153-63.
24. Ayrapetov, M. K.; Nam, N. H.; Ye, G.; Kumar, A.; Parang, K.; Sun, G. Functional diversity of Csk, Chk, and Src SH2 domains due to a single residue variation. *J Biol Chem* **2005**, 280, 25780-7.